

# **Supplemental Material for:**

## **Signatures of post-zygotic structural genetic aberrations in the cells of histologically normal breast tissue that can predispose to sporadic breast cancer**

Lars A. Forsberg, Chiara Rasi, Gyula Pekar, Hanna Davies, Arkadiusz Piotrowski, Devin Absher, Hamid Reza Razzaghian, Aleksandra Ambicka, Krzysztof Halaszka, Marcin Przewoźnik, Anna Kruczak, Geeta Mandava, Saichand Pasupulati, Julia Hacker, K. Reddy Prakash, Ravi Chandra Dasari, Joey Lau, Nelly Penagos-Tafurt, Helena M. Olofsson, Gunilla Hallberg, Piotr Skotnicki, Jerzy Mituś, Jaroslaw Skokowski, Michal Jankowski, Ewa Śrutek, Wojciech Zegarski, Eva Tiensuu Janson, Janusz Ryś, Tibor Tot, and Jan P. Dumanski

Correspondence should be addressed to:

Jan P. Dumanski

Dept. of Immunology, Genetics and Pathology

Uppsala University

Biomedical Center (BMC); B11:4th floor; PO box 815

751 08 Uppsala

Sweden

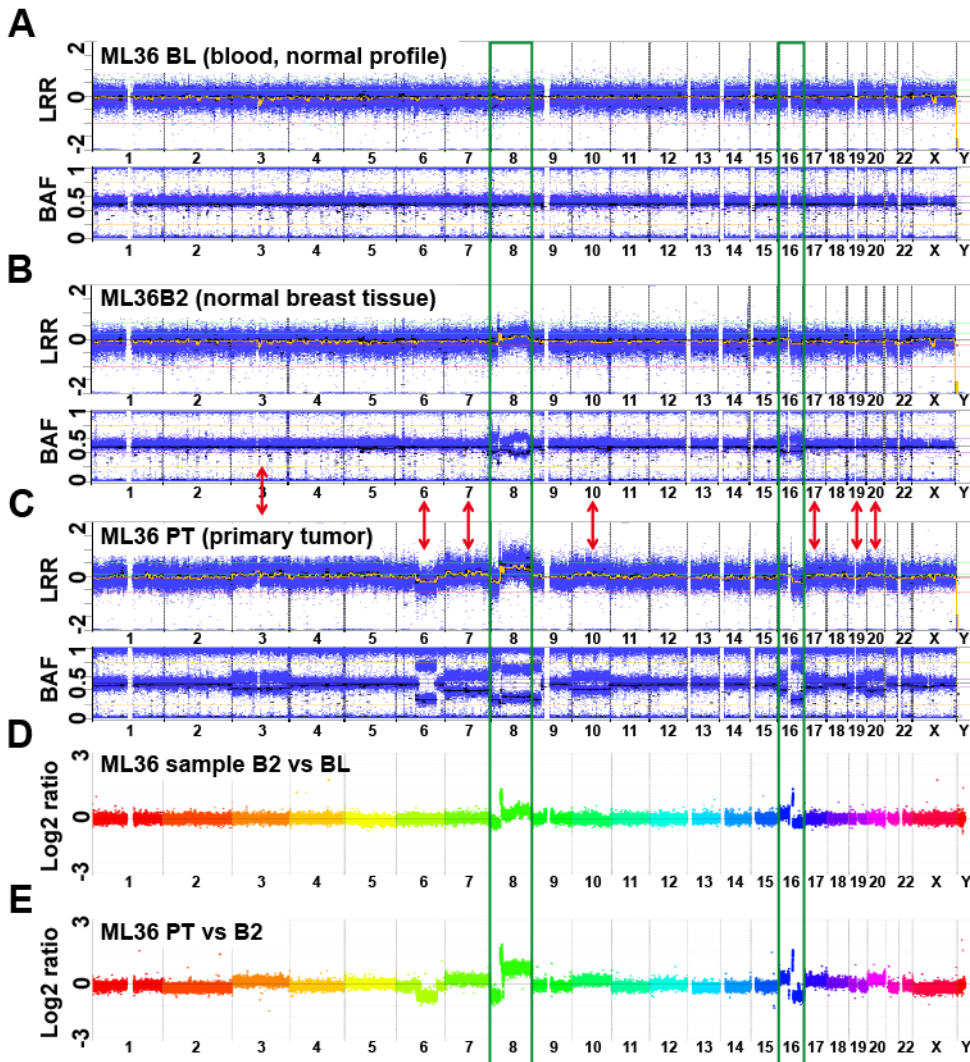
email: [jan.dumanski@igp.uu.se](mailto:jan.dumanski@igp.uu.se) phone: +46 18 471 5035

### **CONTENT:**

**20 Supplemental Figures**

**3 Supplemental Tables**

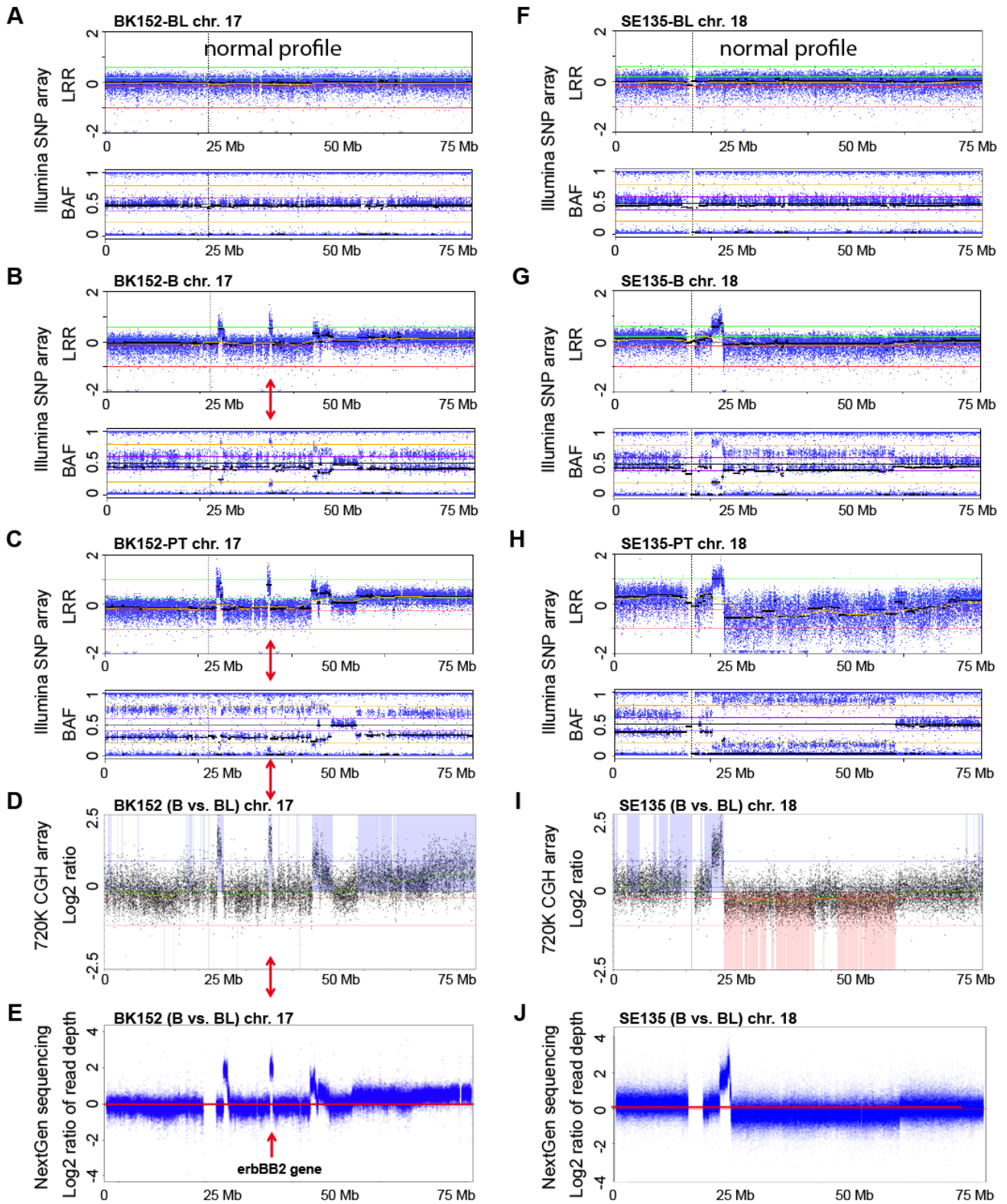
## Supplemental Figure 1



**Supplemental Figure 1.** Validation experiments of structural aberrations detected in UM specimen (ML36B2) and primary tumor (ML36 PT) tissues for the subject ML36 using the NimbleGen 720K array platform. Panels A-C show the whole genome profile from the genotyping of a control sample ML36 BL, ML36B2 and ML36 PT on the Illumina Human1M-Duo platform. Panels D and E show confirmatory array-CGH experiments on Nimblegen 720K chip. Genetic aberrations, characterized by a SNP deviation from the expected Log R ratio (LRR) and B-allele frequency (BAF) values of 0 and 0.5 respectively, were detected on chromosome 8 and 16 in the UM sample (panel B). These regions are highlighted in green in all panels, and as expected tumor sample (panel C and E) show the same aberrations in a higher percentage of cells, and additional changes on other chromosomes (red arrows). No aberrations were detected in blood (panel A).

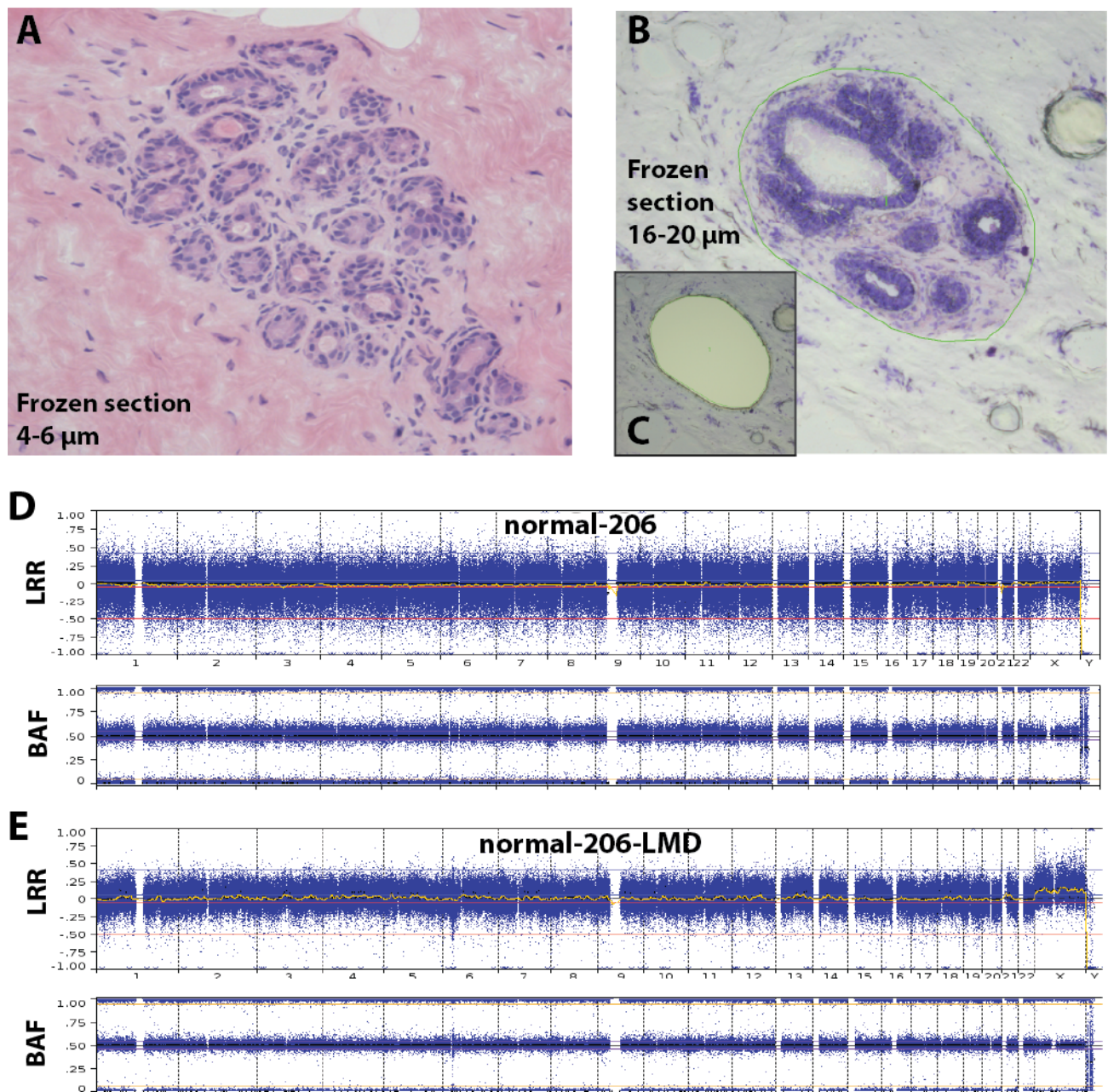
Panels D and E show a comparison between UM and blood (panel D) and PT and blood (panel E) respectively. As shown by the increased Log<sub>2</sub> ratio deviation from 0, the cancer sample harbors a higher number of aberrant cells in comparison to the UM.

## Supplemental Figure 2



**Supplemental Figure 2.** Validation of structural aberrations detected in cases BK152 and SE135 on two distinct additional genome wide analysis platforms. Profiles in A-C and F-H are obtained from genotyping experiments on the Illumina Human1M-Duo BeadChip. Panels D and I display the Log<sub>2</sub> ratio values from confirmatory experiments using the Nimblegen 720K chip in the same chromosomal regions of the panels above. Panels E and J show Log<sub>2</sub> ratio values obtained from the next generation sequencing read depth of the same chromosomes. The results from all platforms show highly concordant results. Structural aberrations detected in the UM of case BK152 (panel B, D and E), including a copy number gain of the well-known breast cancer marker gene *ERBB2* (red arrows), are propagated in the tumor (panel C), but they are not visible in the blood control tissue (panel A), which shows a normal profile. In an analogue manner, copy number changes and allelic imbalances observed on chromosome 18 in the UM of case SE135 (panels G, I and J) are accentuated in the tumor tissue (panel H) and invisible in the blood control from the same subject (panel F).

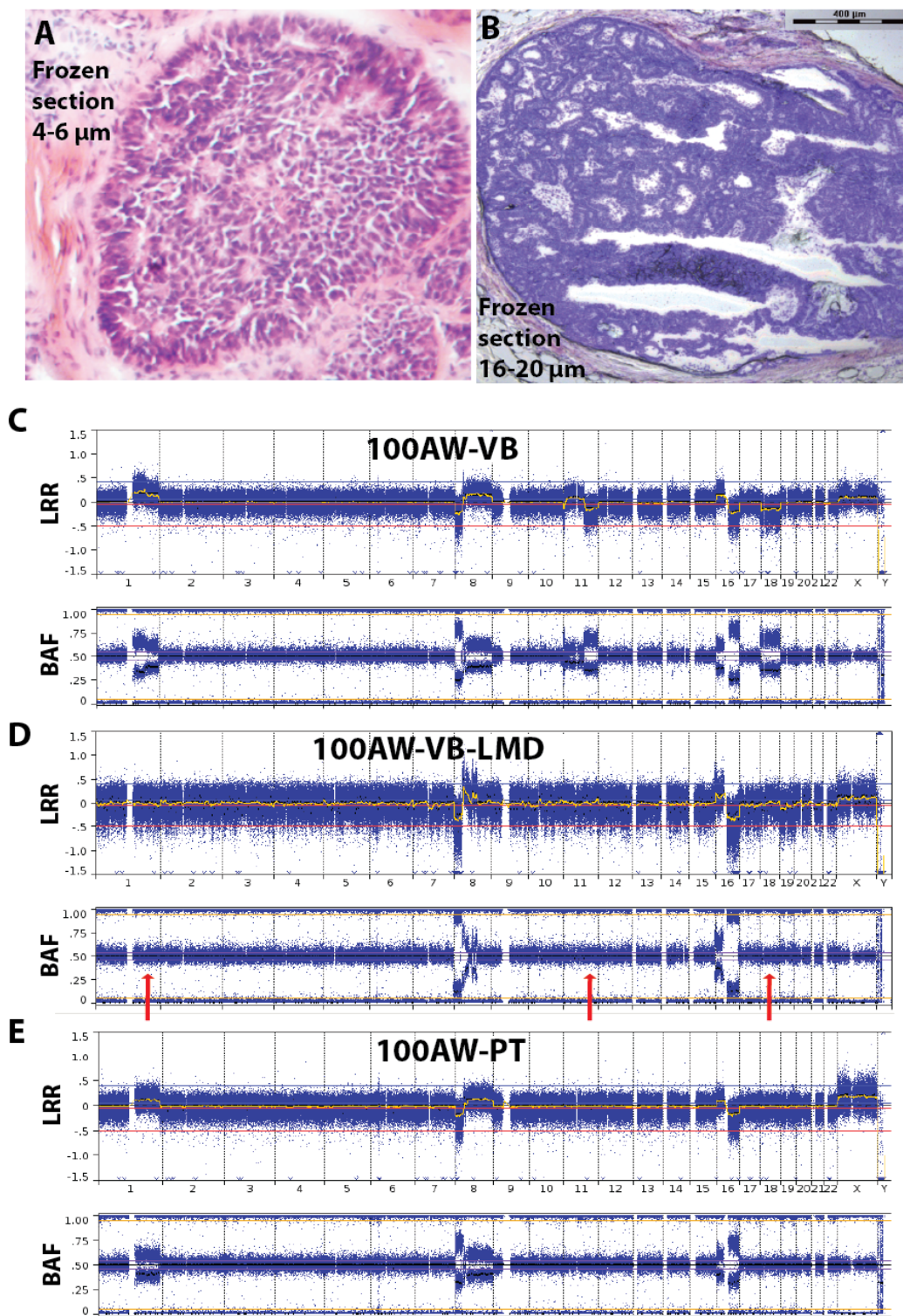
### Supplemental Figure 3



**Supplemental Figure 3.** Test of the methodology for isolation of epithelial cells using laser-micro-dissection (LMD) in a normal specimen of breast parenchyma from plastic surgery (reduction of the breast size) in subject normal-206, followed by Illumina genotyping. Panel A shows a thin (approx. 5 μm) frozen section of hematoxylin and eosin stained normal breast tissue, with histological image of cross-sections through terminal ductal lobular unit (TDLU). Panel B show a thick frozen section (16-20 μm) of cresyl violet stained breast tissue from the same section of breast. Panels B and C display images before and after the LMD cells have

been dissected and collected in a tube underlying the slide. Panels D and E show normal whole-genome profiles using Illumina SNP-array. Panel D has been produced using the DNA derived from a mixture of all cells in sample normal-206, while the profile in panel E is derived from experiment using DNA isolated from micro-dissected cells. The genotyping results from LMD-derived cells in panel E passed all quality control criteria, such as standard deviation of LRR values and the high number of SNP probes that were successfully genotyped (see Materials and Methods-section).

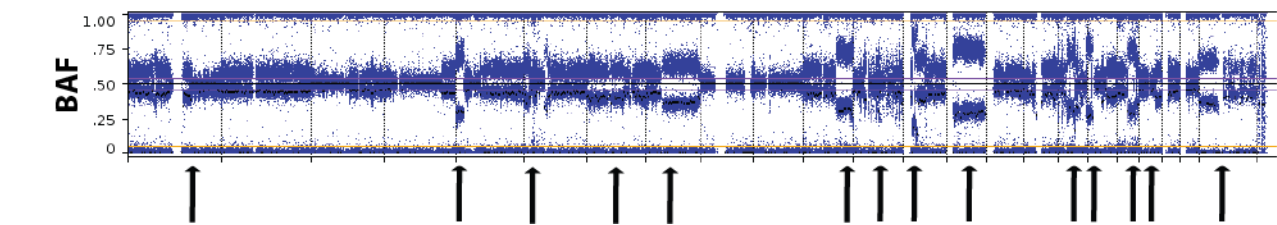
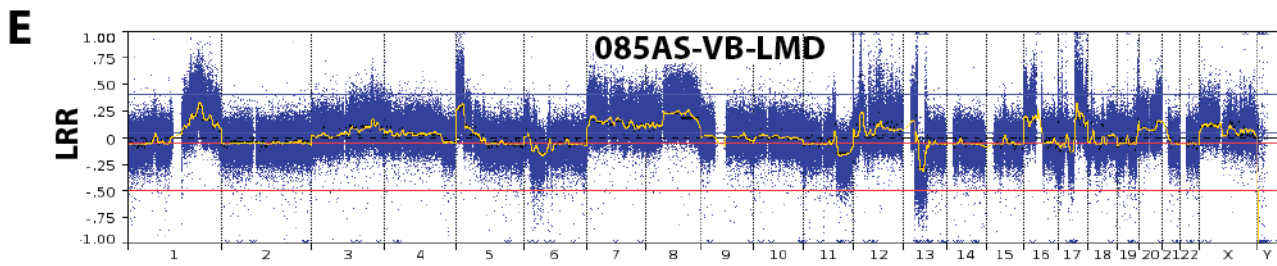
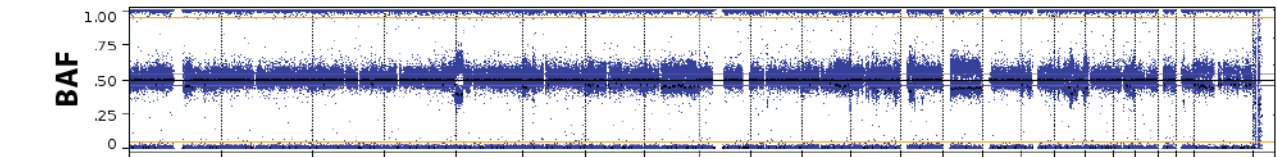
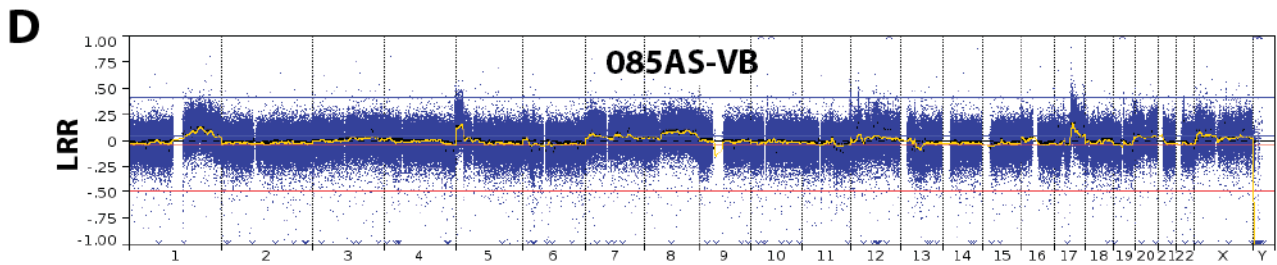
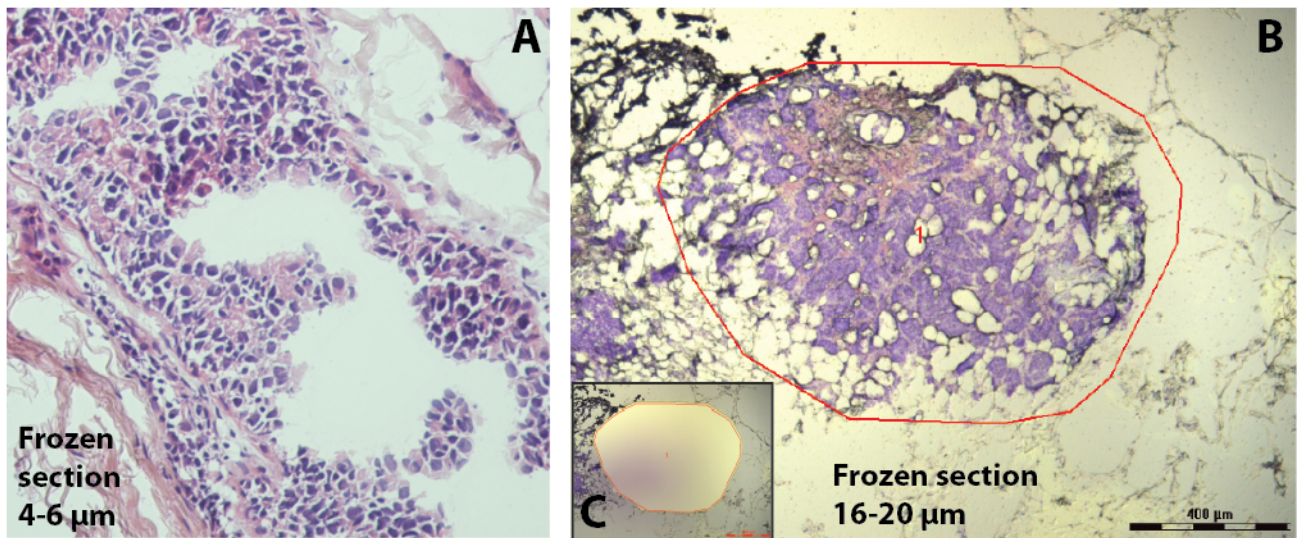
## Supplemental Figure 4



**Supplemental Figure 4.** Validation of detection of structural genetic aberrations in cancer cells after isolation of target cells using laser-micro-dissection (LMD) in case 100AW. Panel A show a thin (4-6  $\mu\text{m}$ ) frozen section of hematoxylin and eosin stained breast tissue with a low grade *in situ* carcinoma that is present

in specimen 100AW-VB. Panel B show a thick frozen section (16-20  $\mu\text{m}$ ) of cresyl violet stained breast tissue from the same specimen 100AW-VB with a low grade *in situ* carcinoma. The entire structure a low-grade cancer from several consecutive slides has been excised with laser. Panels C, D and E show the whole-genome profiles from Illumina SNP-arrays displaying multiple structural genetic aberrations. The genetic profile in panel C has been produced using the bulk DNA derived from mixture of all cells in sample 100AW-VB, while profile in panel D is derived from DNA isolated from LMD-cells. Panel E show the profile derived from DNA isolated from the primary tumor (PT). Some genetic aberrations found in the bulk-DNA are present also in the LMD-cells, and in the PT, for example the 8p- and 16q-deletions. However, red arrows point to some aberrations that are not propagated into the cells isolated in VB-LMD or PT; that is 1q, 11q and chromosome 18. It is noteworthy that primary tumor contains fewer aberrations when compared to bulk DNA derived from 100AW-VB.

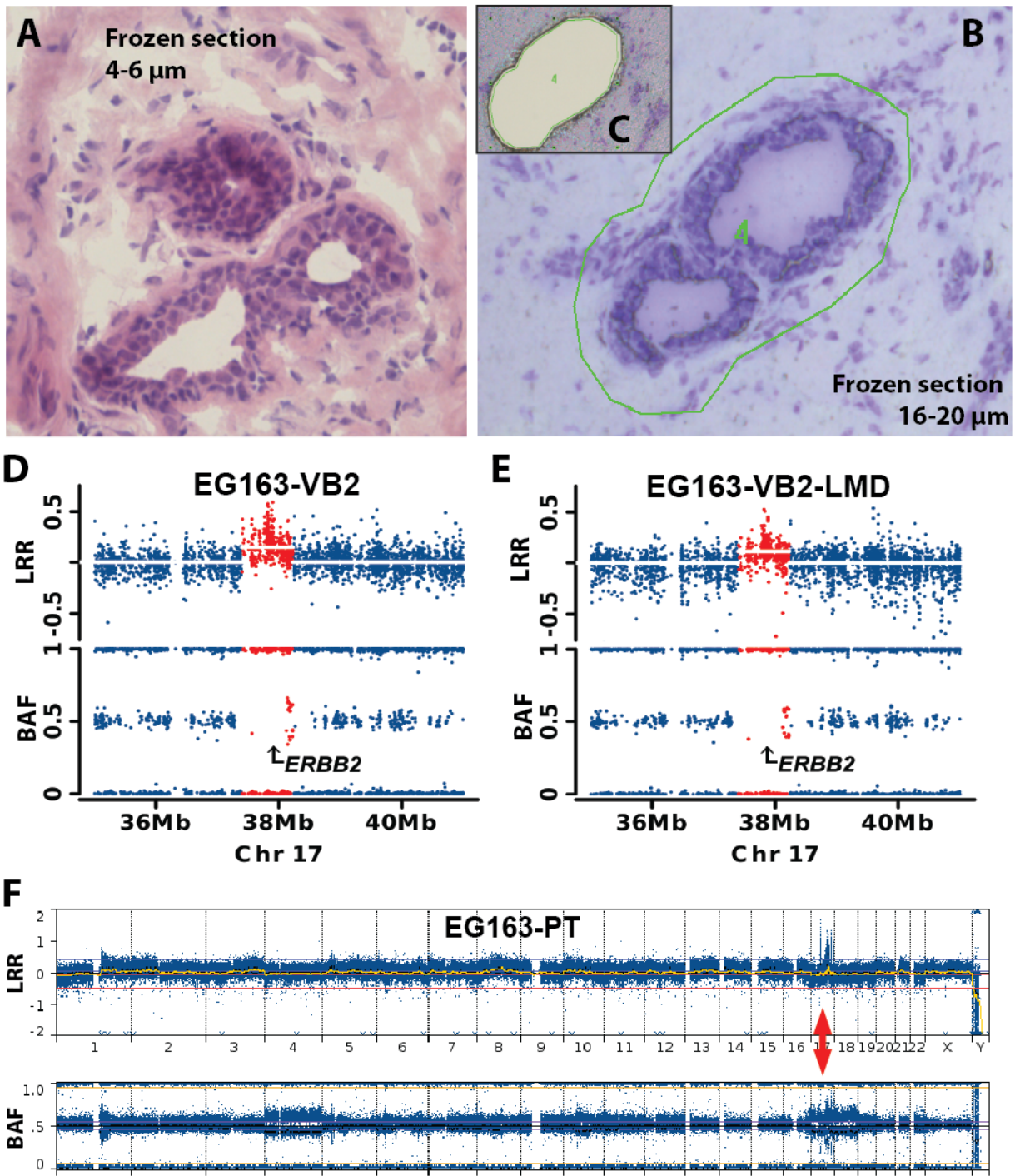
**Supplemental Figure 5**



**Supplemental Figure 5.** Validation of structural genetic aberrations in tumor cells after capturing of the target cells using laser-micro-dissection (LMD) in sample 85AS-VB. Panel A show a thin (4-6  $\mu\text{m}$ ) frozen

section of hematoxylin and eosin stained breast tissue with *in situ* carcinoma in specimen 85AS-VB. Panel B show a thick frozen section (16-20  $\mu\text{m}$ ) of cresyl violet stained breast tissue from the same specimen 85AS-VB with invasive carcinoma. Panels B and C display images before and after the LMD-derived cells have been dissected and collected in a tube underlying the slide. The red irregular circle in panel B shows the area marked for dissection by laser. Panels D and E show the whole-genome profiles from Illumina SNP-arrays displaying multiple structural genetic aberrations. The profile in panel D has been produced using the bulk DNA derived from all cells in sample 85AS-VB, while profile in panel E is derived from DNA isolated from micro-dissected cells. All aberrations found in the analysis of bulk-DNA of sample 85AS-VB are present also in the LMD-treated cells (black arrows), but they were occurring with considerably higher frequency. Many additional aberrations are also visible in the LMD-cells (panel E). In total, the gene copy number imbalances in sample 85AS-VB encompass more than 2/3 of the genome, which is consistent with the aggressive histology pictures in panels A and B.

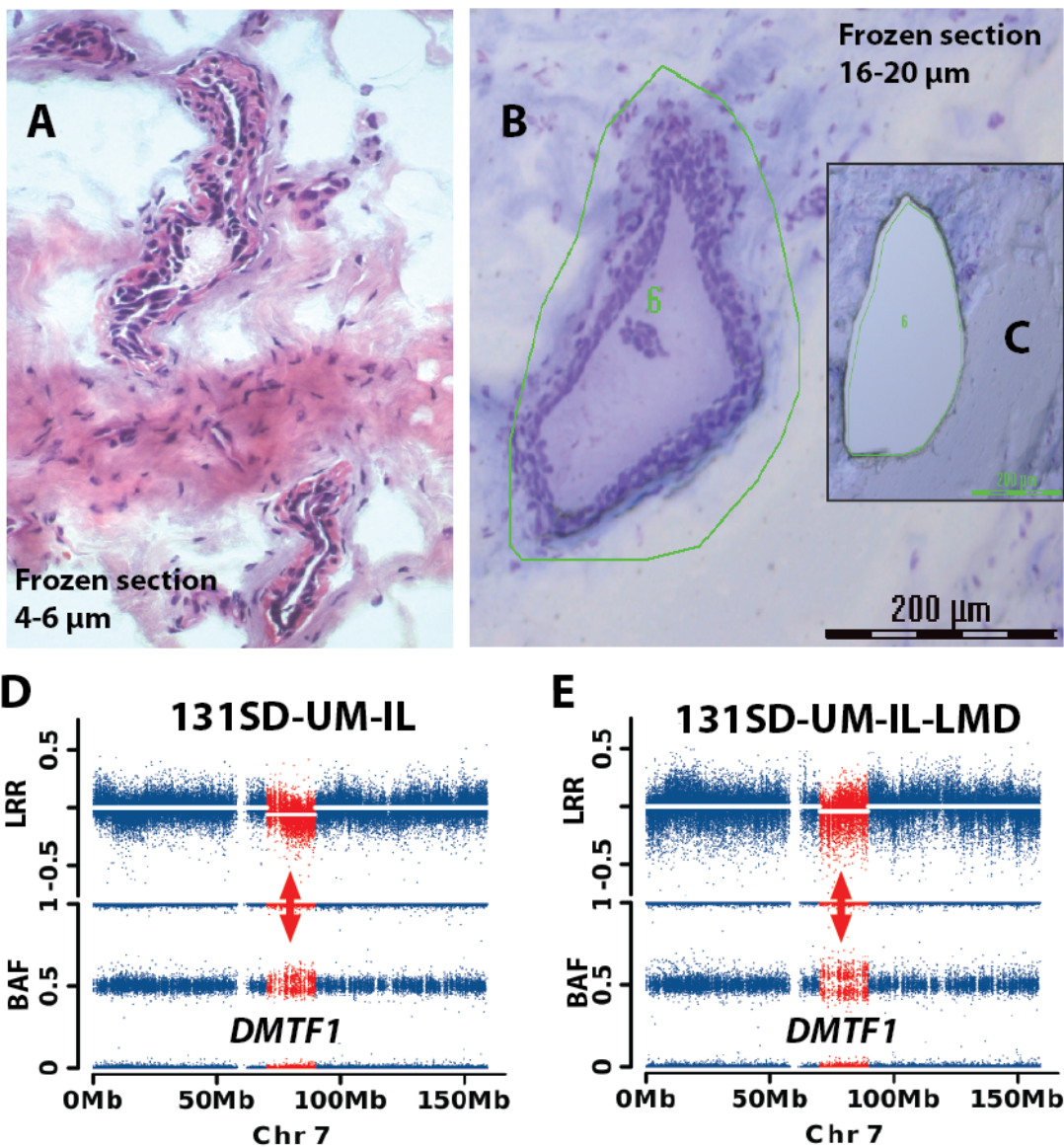
Supplemental Figure 6



**Supplemental Figure 6.** Validation of a gain encompassing the *ERBB2/HER2* gene on 17q in normal epithelial cells by laser-micro-dissection (LMD). Panel A shows a representative image of normal breast parenchyma (hematoxylin and eosin staining) in thin frozen section from specimen EG163-VB2, in which epithelial cells are forming normal ducts. Panels B and C display images before and after the epithelial cells

have been dissected by laser and collected in a tube underlying the slide. The thick frozen section (16-20  $\mu\text{m}$ ) in panel B and C have been stained with cresyl violet. The green irregular circle in panel B shows the area marked for dissection by laser. Panels D and E show the genetic copy number profiles of a part of chromosome 17 from Illumina arrays displaying the gain encompassing the *ERBB2* gene. The arrow indicates the position of the *ERBB2* gene and red segments of the genetic profile are scored as aberrant. The profile in panel D has been produced using the bulk DNA derived from all cells in sample EG163-VB2, while profile in panel E is derived from DNA isolated from micro-dissected epithelial cells. The sample EG163-VB2 shows the *ERBB2* gain present in about 10-15% of cells, as indicated by the BAF values deviating from the value of 0.5. The corresponding number of cells affected by the *ERBB2* gain in sample EG163-VB2-LMD is similar. The total size of aberrations in sample EG163-VB2 is 7.8 Mb. Panel F shows the profile of the corresponding PT sample from case EG163 with pronounced amplification of the *ERBB2* gene (red arrows).

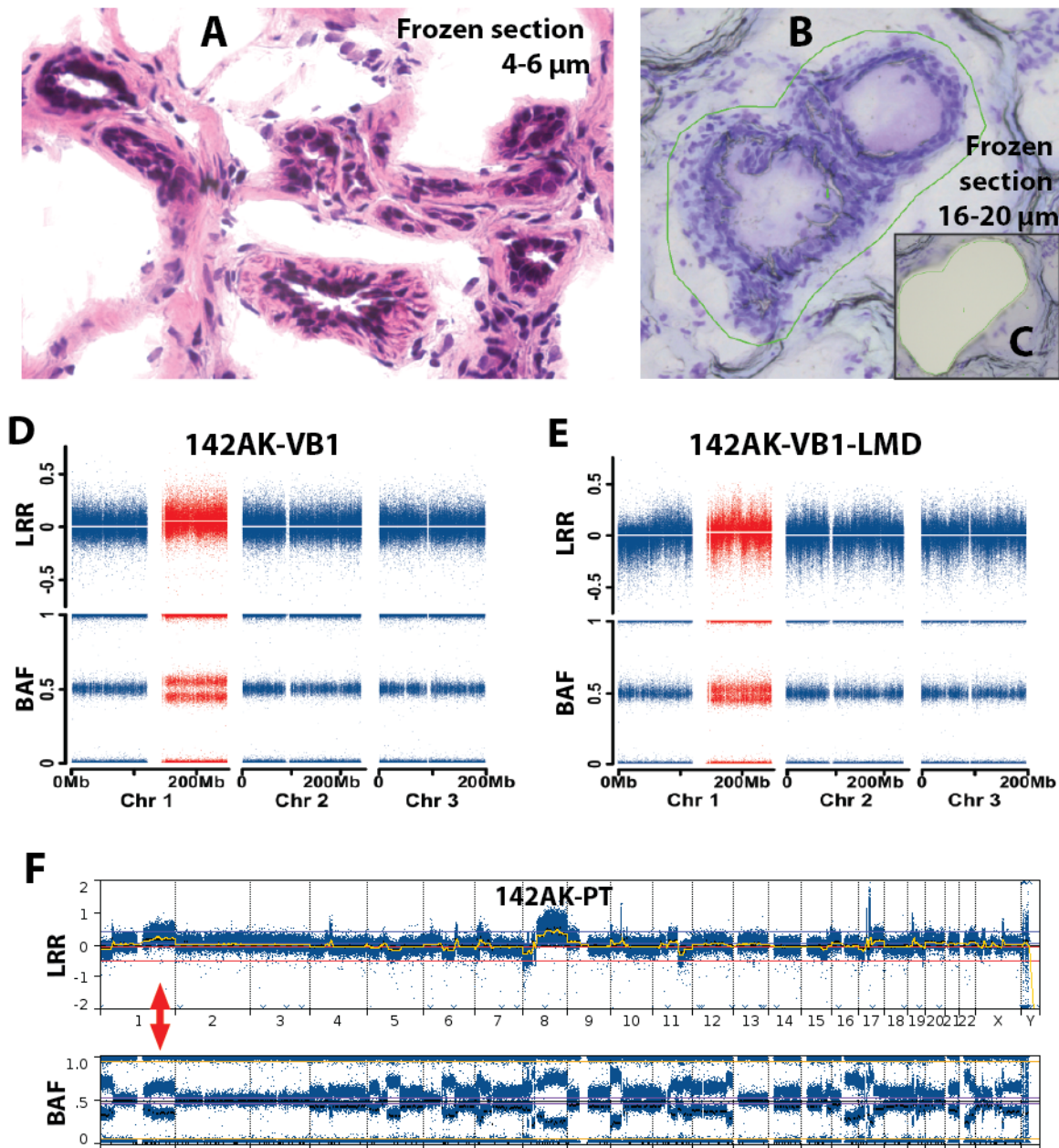
## Supplemental Figure 7



**Supplemental Figure 7.** Validation of a deletion in normal epithelial cells encompassing the Cyclin D Binding Myb-Like Transcription Factor 1 gene (*DMTF1*) by laser-micro-dissection (LMD). Panel A shows a representative image of normal breast parenchyma in hematoxylin and eosin stained thin frozen section from specimen 131SD-UM-IL, in which epithelial cells are forming normal ducts. Panels B and C display images before and after the epithelial cells have been dissected by laser and collected in a tube underlying the slide. The thick frozen section (16-20  $\mu\text{m}$ ) in panel B and C have been stained with cresyl violet. The green irregular circle in panel B shows the area marked for dissection by laser. Panels D and E show the genetic copy number profiles of chromosome 7 from Illumina arrays displaying the deletion encompassing the *DMTF1* gene. The red arrow indicates the position of the *DMTF1* gene and red segments of the genetic profile are scored as

aberrant. Profile in panel D has been produced using the bulk DNA derived from all cells in sample 131SD-UM-IL, while profile in panel E is derived from DNA isolated from micro-dissected epithelial cells. The sample 131SD-UM-IL shows the *DMTF1* deletion present in about 5-10% of cells, as indicated by the BAF values deviating from the value of 0.5. The corresponding number of cells affected by the *DMTF1* deletion in sample 131SD-UM-IL-LMD is 10-20%, suggesting an enrichment of cells with deletion. This deletion of 13.7 Mb on chromosome 7 is the only aberration present in the sample 131SD-UM-IL.

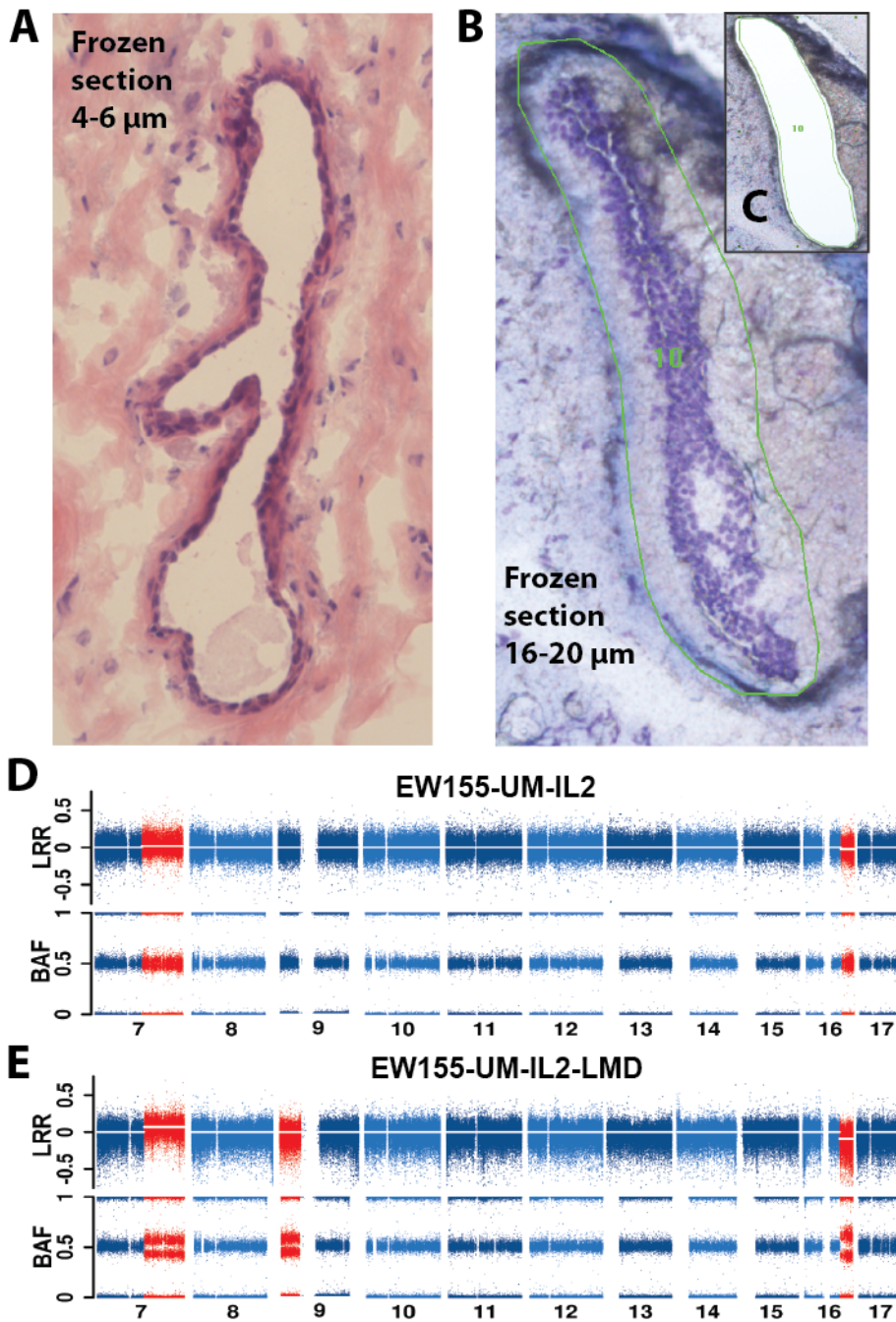
## Supplemental Figure 8



**Supplemental Figure 8.** Laser-micro-dissection (LMD) validation of 1q gain in normal epithelial cells from sample 142AK-VB1. Panel A shows a representative image of normal breast parenchyma (hematoxylin and eosin staining) in thin frozen section from specimen 142AK-VB1, in which epithelial cells are forming normal ducts and lobuli. Panels B and C display images before and after the epithelial cells have been dissected by laser and collected in a tube underlying the slide. The thick frozen section (16-20  $\mu\text{m}$ ) in panel B and C have

been stained with cresyl violet. The green irregular circle in panel B shows the area marked for dissection by laser. Panels D and E show the genetic copy number profiles of chromosomal regions with aberrations (in red) and without (in blue) from Illumina arrays. Profile in panel D has been produced using the bulk DNA derived from all cells in sample 142AK-VB1, while profile in panel E is derived from DNA isolated from micro-dissected epithelial cells. The sample 142AK-VB1 shows 1q gain present in about 10-20% of cells, as indicated by the BAF values deviating from the value of 0.5. The corresponding number of cells affected by the 1q-gain in sample 142AK-VB1-LMD is slightly lower. The size of the 1q-gain in sample 142AK-VB1 is 105.6 Mb and this is the only detectable aberration in this sample. Panel F shows the profile from Illumina experiment for the primary tumor (142AK-PT), displaying that the chromosome 1 aberration (red arrow) is propagated into the tumor and that the 1q-gain is present in approx. 40-60% of cells. The tumor contains numerous additional aberrations, with more than 2/3 of the genome displaying copy number changes.

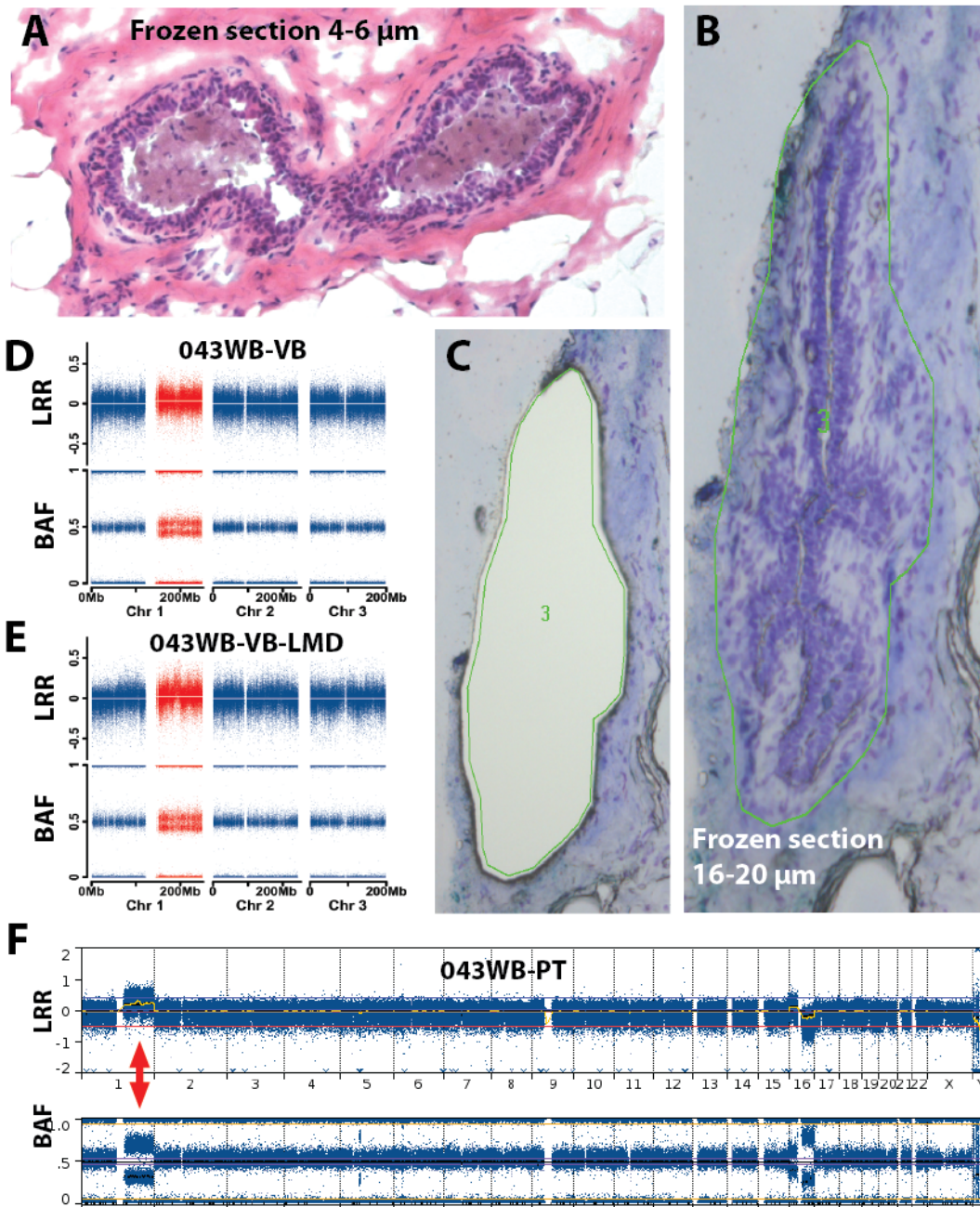
## Supplemental Figure 9



**Supplemental Figure 9.** Laser-micro-dissection (LMD) validation of a gain on 7q and deletion on 16q present in normal epithelial cells from sample EW155-UM-IL2. Panel A shows a representative image of normal breast parenchyma (hematoxylin and eosin staining) in thin frozen section from specimen EW155-UM-IL2, in which epithelial cells are forming a normal duct. Panels B and C display images before and after the

epithelial cells have been dissected by laser and collected in a tube underlying the slide. The thick frozen section (16-20  $\mu\text{m}$ ) in panel B and C have been stained with cresyl violet. The green irregular circle in panel B shows the area marked for dissection by laser. Panels D and E show the genetic copy number profiles of chromosomes with aberrations (in red) and without (in blue) from Illumina arrays. Profile in panel D has been produced using the bulk DNA derived from all cells in sample EW155-UM-IL2, while profile in panel E is derived from DNA isolated from micro-dissected epithelial cells. The sample EW155-UM-IL2 shows a gain on 7q and deletion on 16q present in about 5-15% of cells, as indicated by the BAF values deviating from the value of 0.5. The corresponding number of cells affected by deletions in sample EW155-UM-IL2-LMD is higher (10-20%), suggesting an enrichment of cells with aberrations. The combined load of aberrations on chromosome 7 and 16 in the sample EW155-UM-IL2 is 98.6 Mb. Remarkably, micro-dissected sample EW155-UM-IL2-LMD also contains approx. 10-20% of cells with a copy number neutral loss of heterozygosity (CNN-LOH) of 9p, which was not detectable in the bulk DNA derived from all cells in sample EW155-UM-IL2.

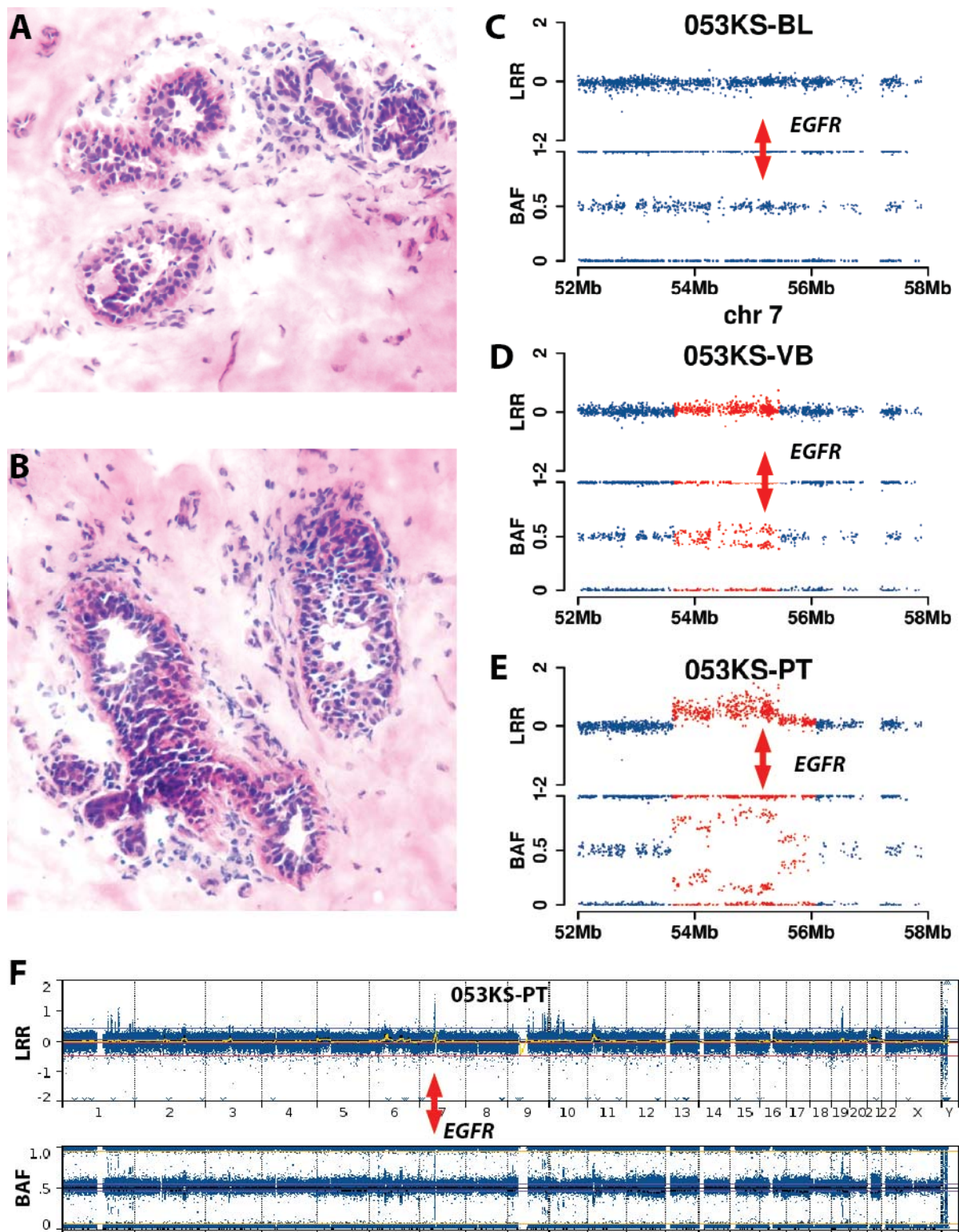
Supplemental Figure 10



**Supplemental Figure 10.** Laser-micro-dissection (LMD) validation of the 1q gain in normal epithelial cells from sample 043WB-VB. Panel A shows a representative image of normal breast parenchyma (hematoxylin and eosin staining) in thin frozen section from specimen 043WB-VB, in which epithelial cells are forming normal ducts. Panels B and C display images before and after the epithelial cells have been dissected by laser and collected in a tube underlying the slide. The thick frozen section (16-20  $\mu\text{m}$ ) in panel B and C have been stained with cresyl violet. The green irregular circle in panel B shows the area marked for dissection by laser.

Panels D and E show the genetic copy number profiles of chromosomal regions with aberrations (in red) and without (in blue) from Illumina arrays. Profile in panel D has been produced using the bulk DNA derived from all cells in sample 043WB-VB, while profile in panel E is derived from DNA isolated from micro-dissected epithelial cells. The sample 043WB-VB shows a 1q gain present in about 5-15% of cells, as indicated by the BAF values deviating from the value of 0.5. The corresponding number of cells affected by the 1q-gain in sample 043WB-VB-LMD is similar. The size of the 1q aberration in sample 043WB-VB is 105.6 Mb. Panel F shows the profile from SNP-array for the primary tumor (043WB-PT), in which the chromosome 1 aberration (red arrow) is propagated in PT and is present in approx. 30-50% of cells. The tumor contains also additional aberrations on chromosome 5 and 16.

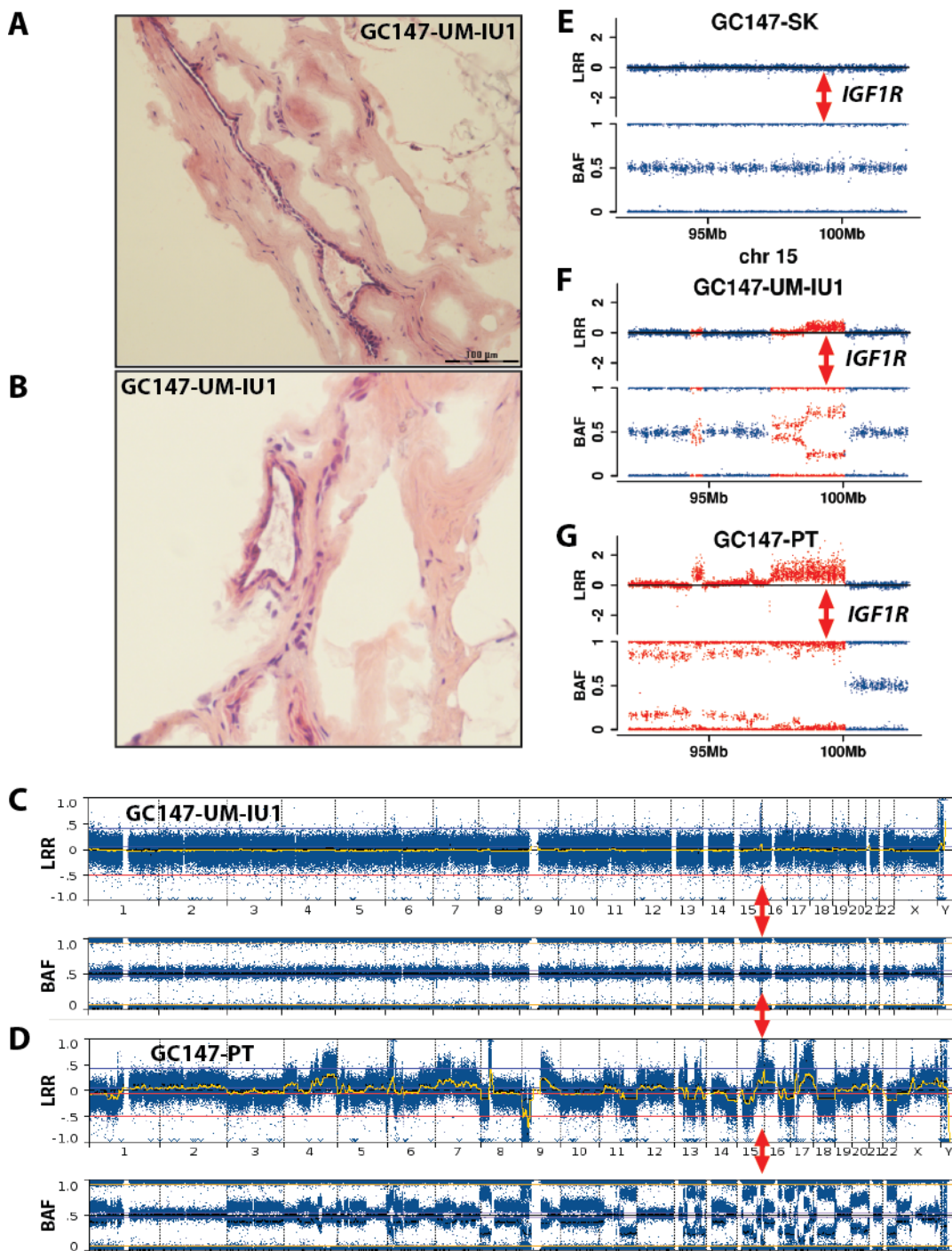
## Supplemental Figure 11



**Supplemental Figure 11.** Normal breast tissue in sample VB from case 053KS shows increased gene copy number of the Epidermal Growth Factor Receptor (*EGFR*) gene. Panels A and B show representative images

of breast parenchyma in hematoxylin and eosin stained frozen sections (approx. 5  $\mu$ m) from specimen 053KS-VB, in which epithelial cells are forming ducts. As shown in panel B, this specimen in addition to normal ducts, contained small ducts with mild epithelial hyperplasia. Atypia, *in situ* carcinoma or invasive carcinoma was not detected by histological analysis of this specimen. Panels C, D and E show details of SNP-array for the region on chromosome 7 containing *EGFR* (red arrows) from analysis of blood (BL, normal control tissue), normal breast tissue from the sample VB and primary tumor (PT), respectively. As expected, sample BL shows a normal profile in panel C. Genomic segments in red in panels D and E were scored as abnormal in copy number and/or allelic ratio. The sample VB shows a single copy gain of the *EGFR* gene present in about 5-15% of cells, as indicated by the BAF values deviating from the value of 0.5. In primary tumor sample, the number of cells with a gain of *EGFR* is 75-90%. Panel F shows whole genome profile from Illumina arrays for PT sample, which contains many additional aberrations throughout the genome. The position of the *EGFR* gene is denoted by a red arrow. The total size of aberrations in sample 053KS-VB is 1.8 Mb.

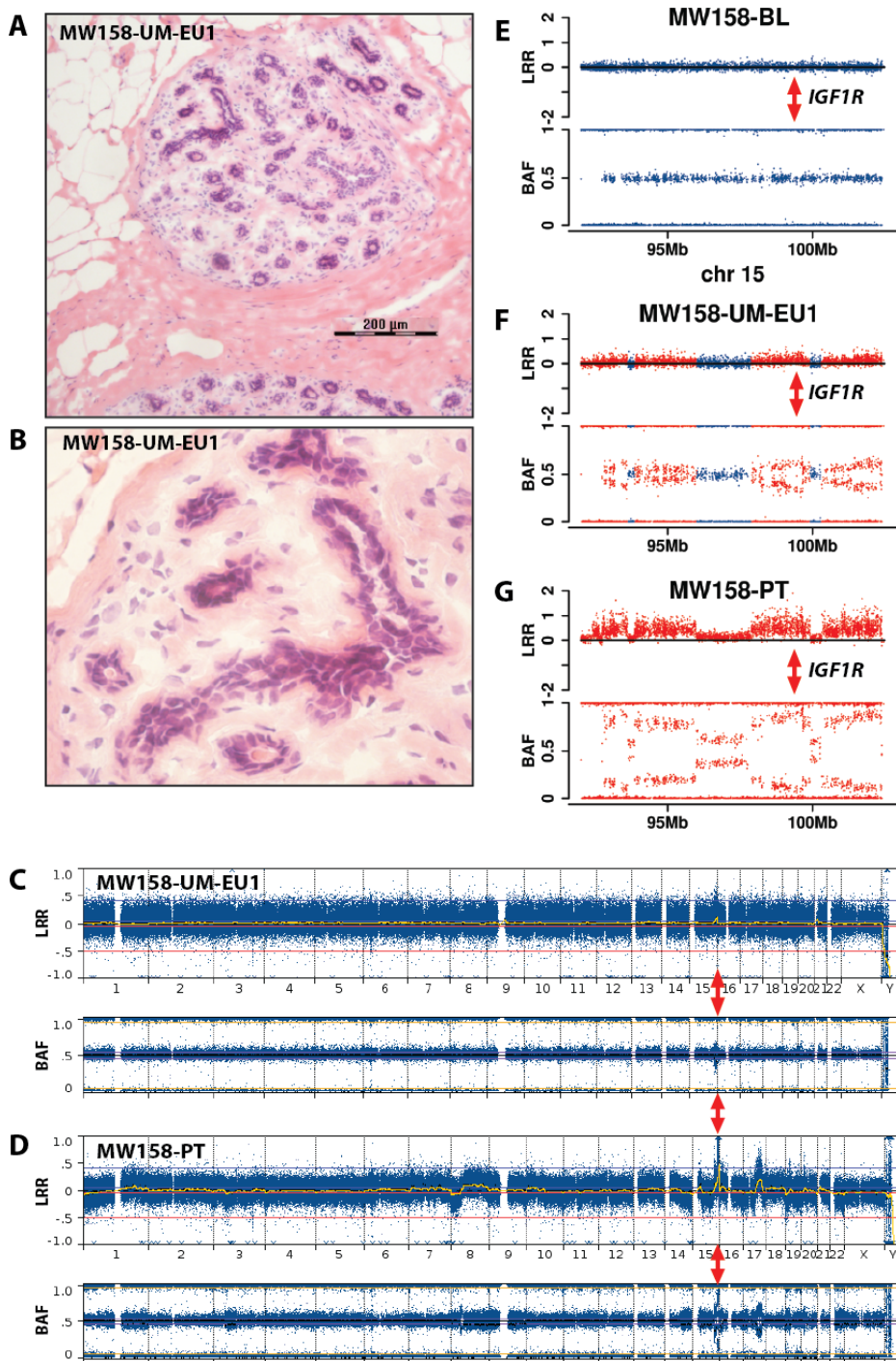
**Supplemental Figure 12**



**Supplemental Figure 12.** Normal breast tissue in sample UM-IU1 from case GC147 shows considerably increased gene copy number of the Insulin-Like Growth Factor 1 Receptor (*IGF1R*) gene. Panels A and B show representative images of normal breast parenchyma in hematoxylin and eosin stained frozen sections (approx. 5  $\mu$ m) from specimen UM-IU1, in which epithelial cells are forming normal ducts. Detailed histological analysis showed no atypical cells in the sample. Panels C and D show whole genome profiles

from SNP-arrays for the UM sample of histologically normal breast tissue and primary tumor from this case, respectively. The genomic copy-number profile of sample UM-IU1 is normal, except for a pronounced copy number gain of *IGF1R*. Primary tumor in panel D shows numerous aberrations throughout the genome, involving more than half of the chromosomes. The position of the *IGF1R* gene is denoted by red arrows. Panels E, F and G show the details of Illumina genotyping for the region on 15q containing the *IGF1R* gene (red arrows) from analysis of skin (SK, normal control tissue), normal breast tissue from the sample UM-IU1 and primary tumor, respectively. As expected, sample SK show normal profile in panel E. Genomic segments in red in panels F and G were scored as abnormal in copy number and/or allelic ratio. The sample UM-IU1 shows a single copy gain of the *IGF1R* gene present in about 40-60% of cells, as indicated by the BAF values deviating from the value of 0.5. In primary tumor sample, the number of cells with a gain of the *IGF1R* gene is close to 100%. The total size of aberrations in sample GC147-UM-IU1 is 2.9 Mb.

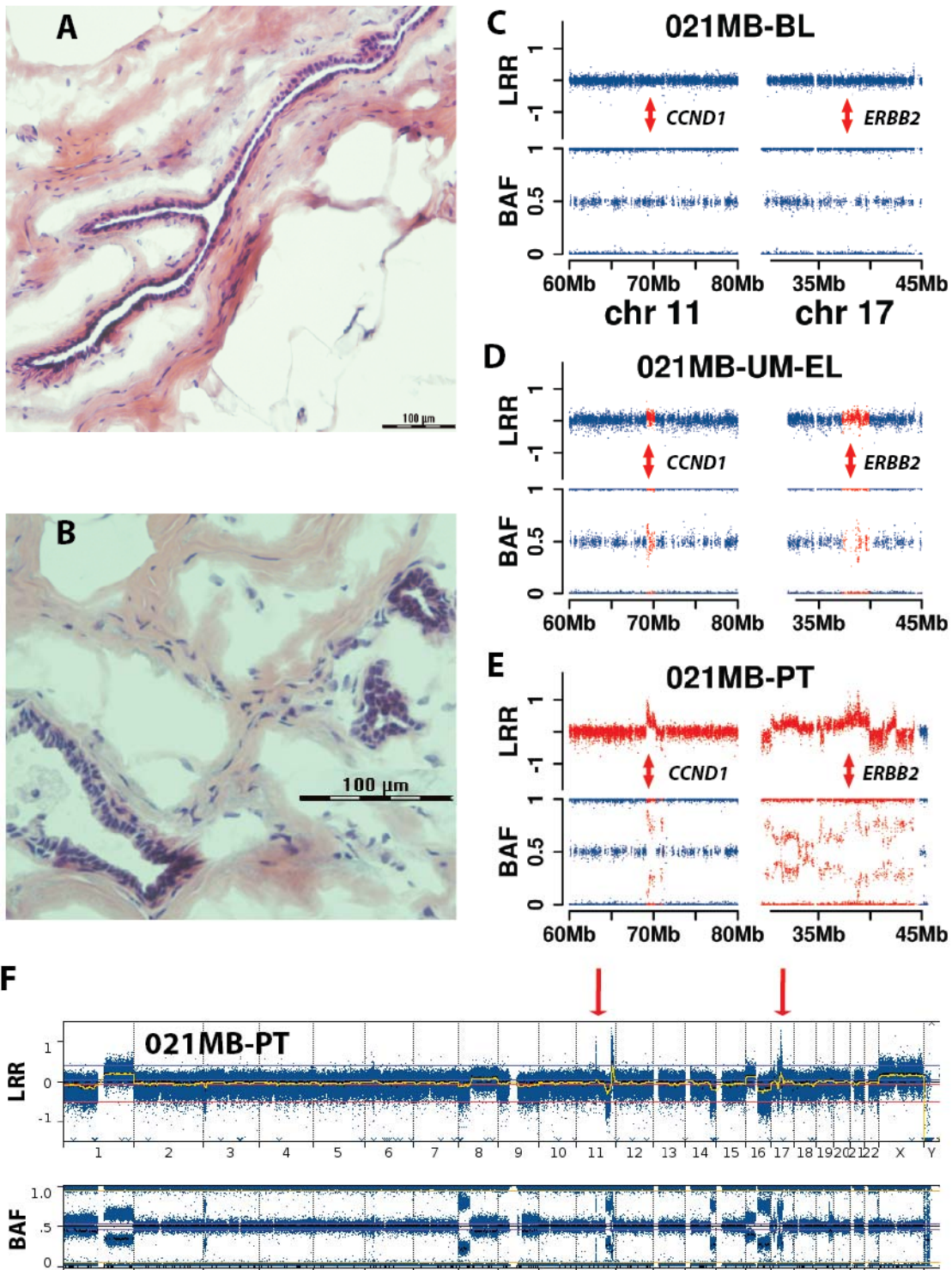
Supplemental Figure 13



**Supplemental Figure 13.** Normal breast tissue in sample UM-EU1 from case MW158 show increased gene copy number of the Insulin-Like Growth Factor 1 Receptor (*IGF1R*) gene. Panels A and B show representative images of normal breast parenchyma in hematoxylin and eosin stained frozen sections (approx. 5 μm) from specimen UM-EU1, in which epithelial cells are forming normal ductules and terminal ductal lobular units (TDLUs). Detailed histological analysis showed no atypical cells in the sample. Panels C and D show whole genome profiles from Illumina arrays for UM sample of normal breast tissue and primary tumor

from this case, respectively. The genomic copy-number profile of sample UM-EU1 is normal, except for a copy number gain of the *IGF1R* gene. Primary tumor in panel D shows numerous aberrations through the genome. The position of the *IGF1R* gene is denoted by red arrows. Panels E, F and G show the details of Illumina genotyping for the region on 15q containing the *IGF1R* gene (red arrows) from analysis of blood (BL, normal control tissue), normal breast tissue from the sample UM-EU1 and primary tumor, respectively. As expected, sample BL show normal profile in panel E. Genomic segments in red in panels F and G were scored as abnormal in copy number and/or allelic ratio. The sample UM-EU1 shows a single copy gain of the *IGF1R* gene present in about 25-40% of cells, as indicated by the BAF values deviating from the value of 0.5. In primary tumor, the number of cells with a gain of the *IGF1R* gene is 80-95%. The total size of aberrations in sample MW158-UM-EU1 is 7.4 Mb.

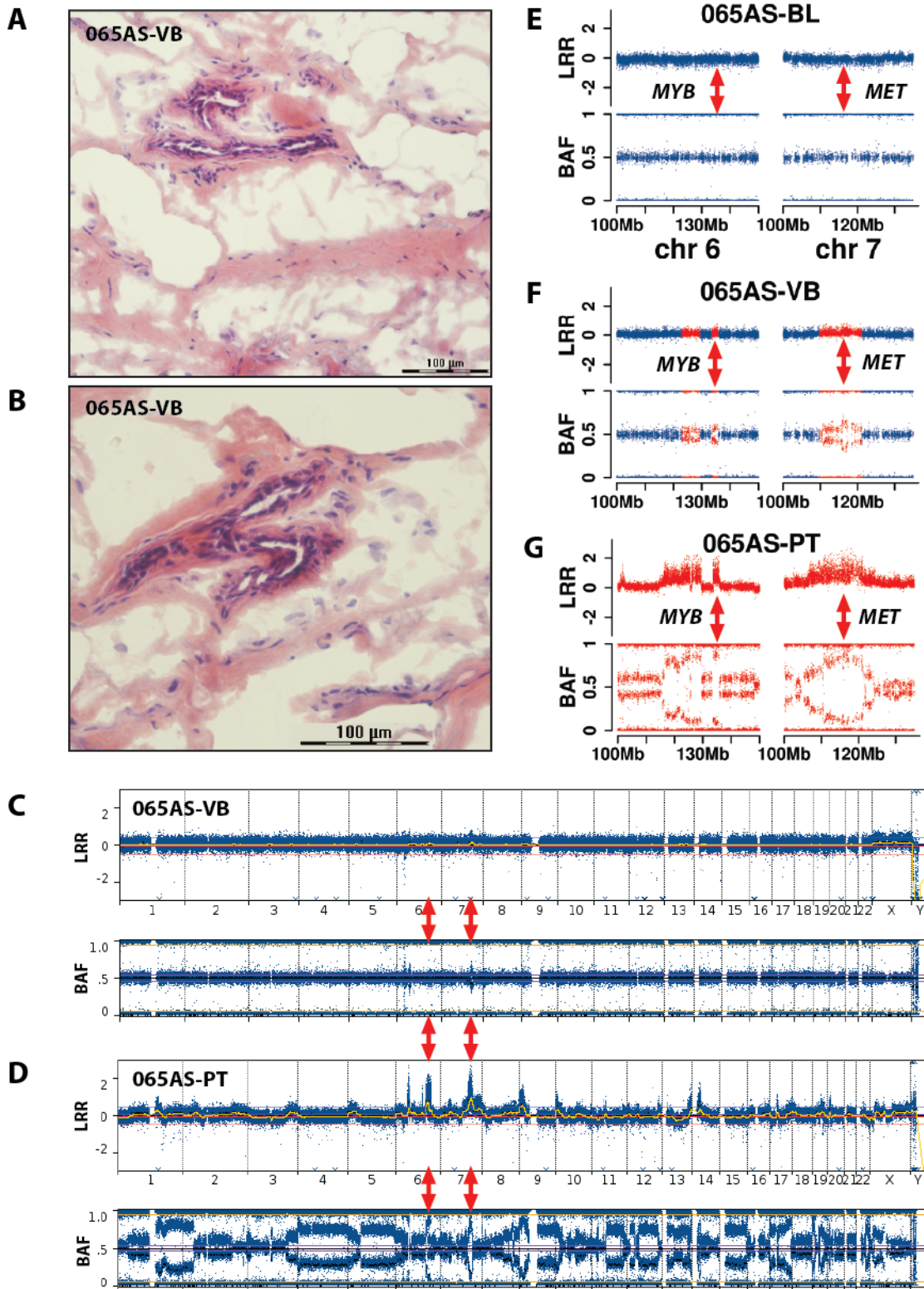
Supplemental Figure 14



**Supplemental Figure 14.** Normal breast tissue in sample UM-EL from case 021MB shows an increased copy number of the *CCND1* and *ERBB2* genes (red arrows). Panels A and B show representative images of normal breast parenchyma in hematoxylin and eosin stained frozen sections (approx. 5  $\mu$ m) from specimen UM-EL, in which epithelial cells are forming normal ducts. Detailed histological analysis showed no atypical

cells in the sample. Panels C, D and E show details of the Illumina genotyping for samples 021MB-blood, 021MB-UM-EL and 021MB-PT, respectively, from chromosome 11 (covering the *CCND1* locus) and 17 (the *ERBB2* locus). Panel F displays whole genome profile from Illumina array for PT sample. The genomic copy-number profile of sample UM-EL is normal, except for discrete copy number gains of the *CCND1* and *ERBB2* genes. The primary tumor in panel F shows multiple additional aberrations. As expected, control sample BL shows a normal profile in panel C. Genomic segments in red in panels D and E were scored as abnormal in copy number and/or allelic ratio. The sample UM-EL shows a gain of the *CCND1* and *ERBB2* genes present in about 5-10% of cells, as clearly indicated by the BAF values deviating from the value of 0.5. In primary tumor sample, the number of cells with gains of the *CCND1* and *ERBB2* genes is in the range of 70-90%. The total size of aberrations in sample 021MB-UM-EL is 8.1 Mb.

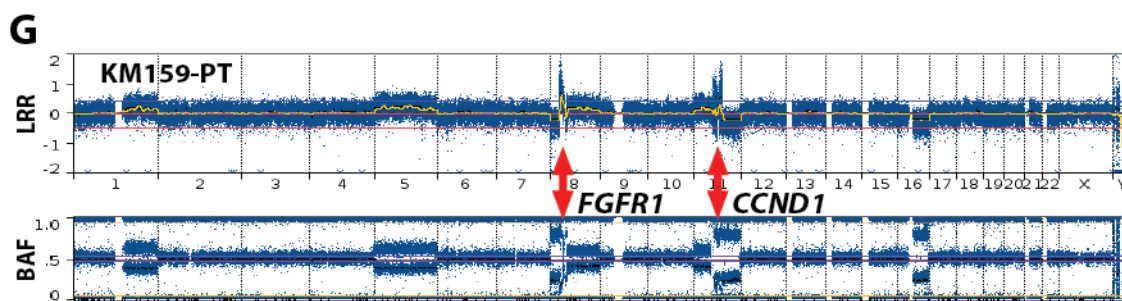
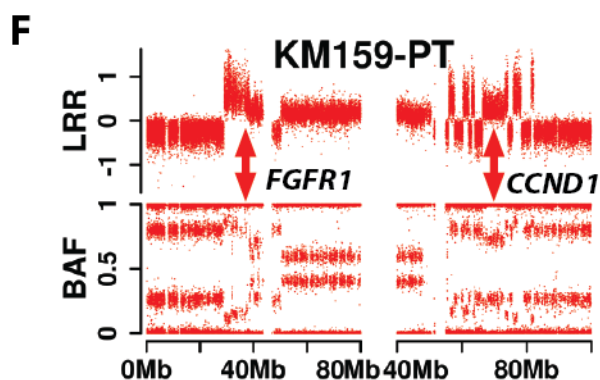
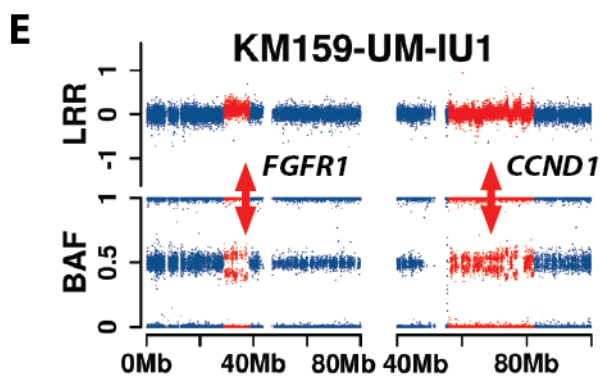
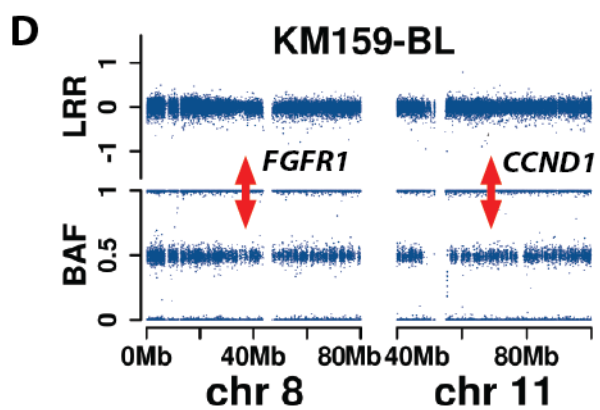
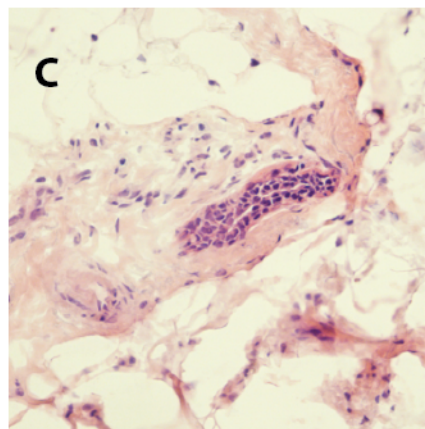
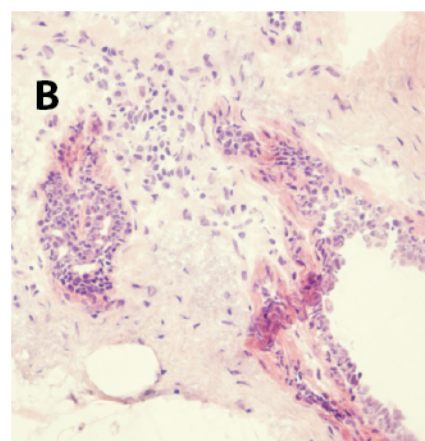
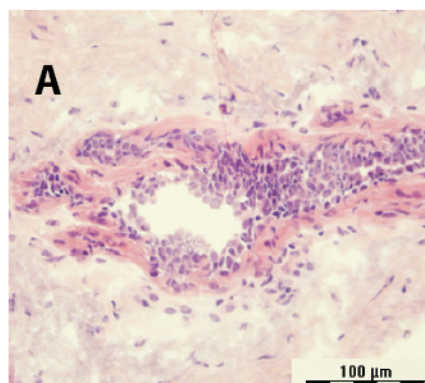
Supplemental Figure 15



**Supplemental Figure 15.** Normal breast tissue in a sample VB from case 065AS shows increased gene copy number of the *MYB* and *MET* proto-oncogenes. Panels A and B show representative images of normal breast

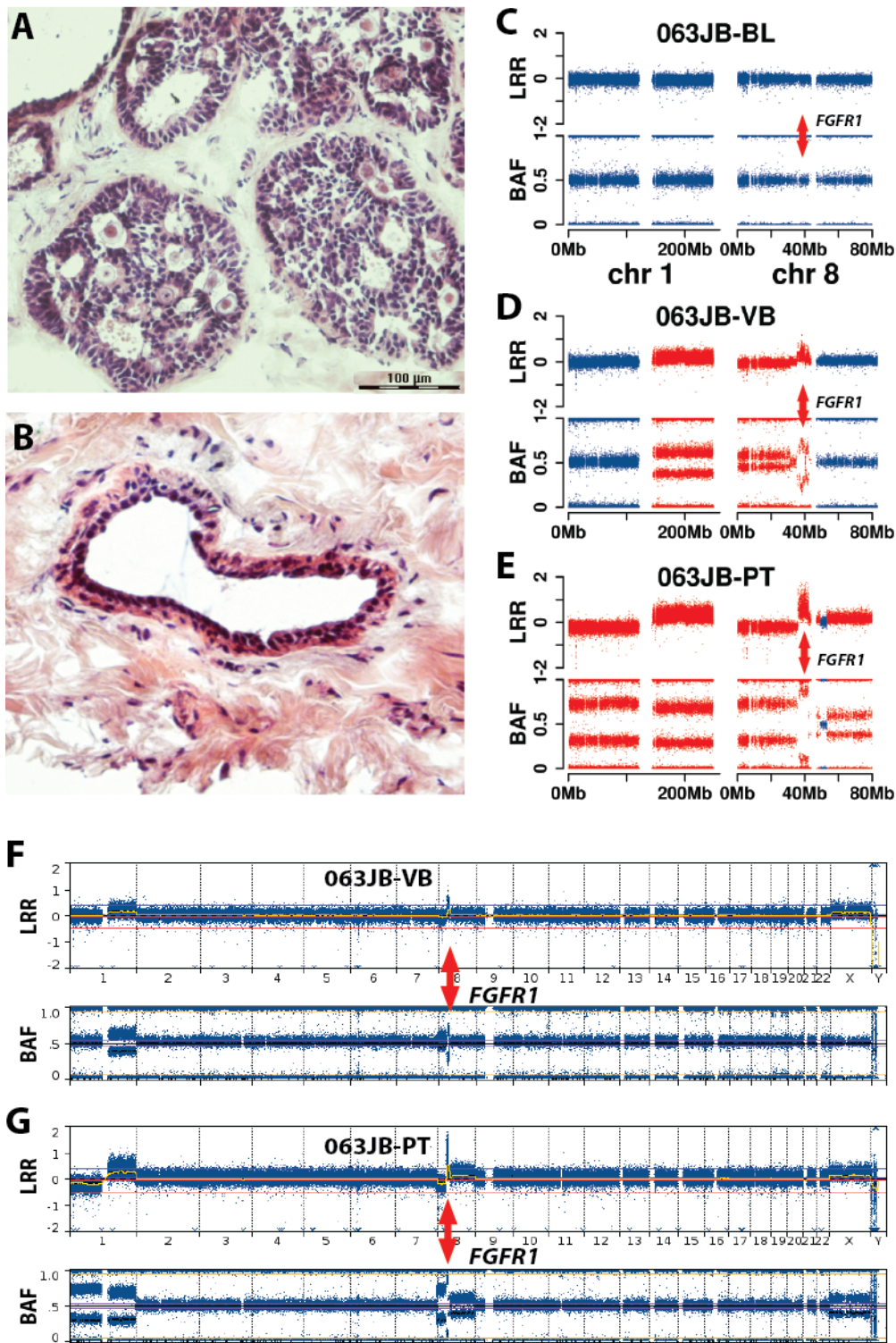
parenchyma in hematoxylin and eosin stained frozen sections (approx. 5  $\mu\text{m}$ ) from specimen VB, in which epithelial cells are forming normal ducts. Detailed histological analysis showed no atypical cells in the sample. Panels C and D show whole genome profiles from SNP-arrays for VB sample of normal breast tissue and primary tumor from this case, respectively. The genomic copy-number profile of sample VB is normal, except for the copy number gains of the *MYB* and *MET* proto-oncogenes (red arrows). Primary tumor in panel D shows numerous aberrations encompassing more than two-thirds of the genome. Panels E, F and G show the details of Illumina genotyping for the region on chromosome 6 and chromosome 7 containing the *MYB* and *MET* genes (red arrows) from analysis of blood (BL, normal control tissue), normal breast tissue (VB) and primary tumor, respectively. As expected, sample BL show normal profile in panel E. Genomic segments in red in panels F and G were scored as abnormal in copy number and/or allelic ratio. The sample VB shows a gain of the *MYB* gene present in about 5-10% of cells, as indicated by the BAF values deviating from the value of 0.5. The corresponding number of cells affected by a single copy gain of *MET* gene region is 10-20%. In primary tumor sample, the number of cells with a gain of the *MYB* and *MET* proto-oncogenes is close to 100%. The total size of aberrations in sample 065AS-VB is 46.3 Mb.

Supplemental Figure 16



**Supplemental Figure 16.** Normal breast tissue in a sample UM-IU1 from case KM159 shows increased copy number of the *FGFR1* and *CCND1* genes. Panels A, B and C show representative images of normal breast parenchyma in hematoxylin and eosin stained frozen sections (approx. 5  $\mu$ m) from specimen UM-IU1, with normal ducts. As shown in panel A and B but not C, this UM-IU1 specimen in addition to normal ducts, contained ducts with mild epithelial hyperplasia. Atypical, *in situ* carcinoma or invasive carcinoma cells were not detected by histological analysis. Panels D, E and F show the details of Illumina profile for the regions on chromosome 8 and chromosome 11, containing *FGFR1* and *CCND1* (red arrows) in blood (BL, normal control tissue), normal breast tissue from the sample UM-IU1 and primary tumor, respectively. As expected, sample BL show normal profile (panel D). Genomic segments in red (panels E and F) were scored as abnormal in copy number and allelic ratio. The sample UM-IU1 shows a gain of *FGFR1* and *CCND1* genes present in about 10-15% of cells, as indicated by the BAF values deviating from the value of 0.5. In PT sample, the number of cells with a gain of the *FGFR1* and *CCND1* genes is 70-90%. The total size of all aberrations present in UM-IU1 specimen is 173.1 Mb, the highest in all studied samples, still having a normal histological appearance. Panel G shows the whole genome profile for PT, which has multiple additional aberrations. The position of the *FGFR1* and *CCND1* genes is denoted by red arrows.

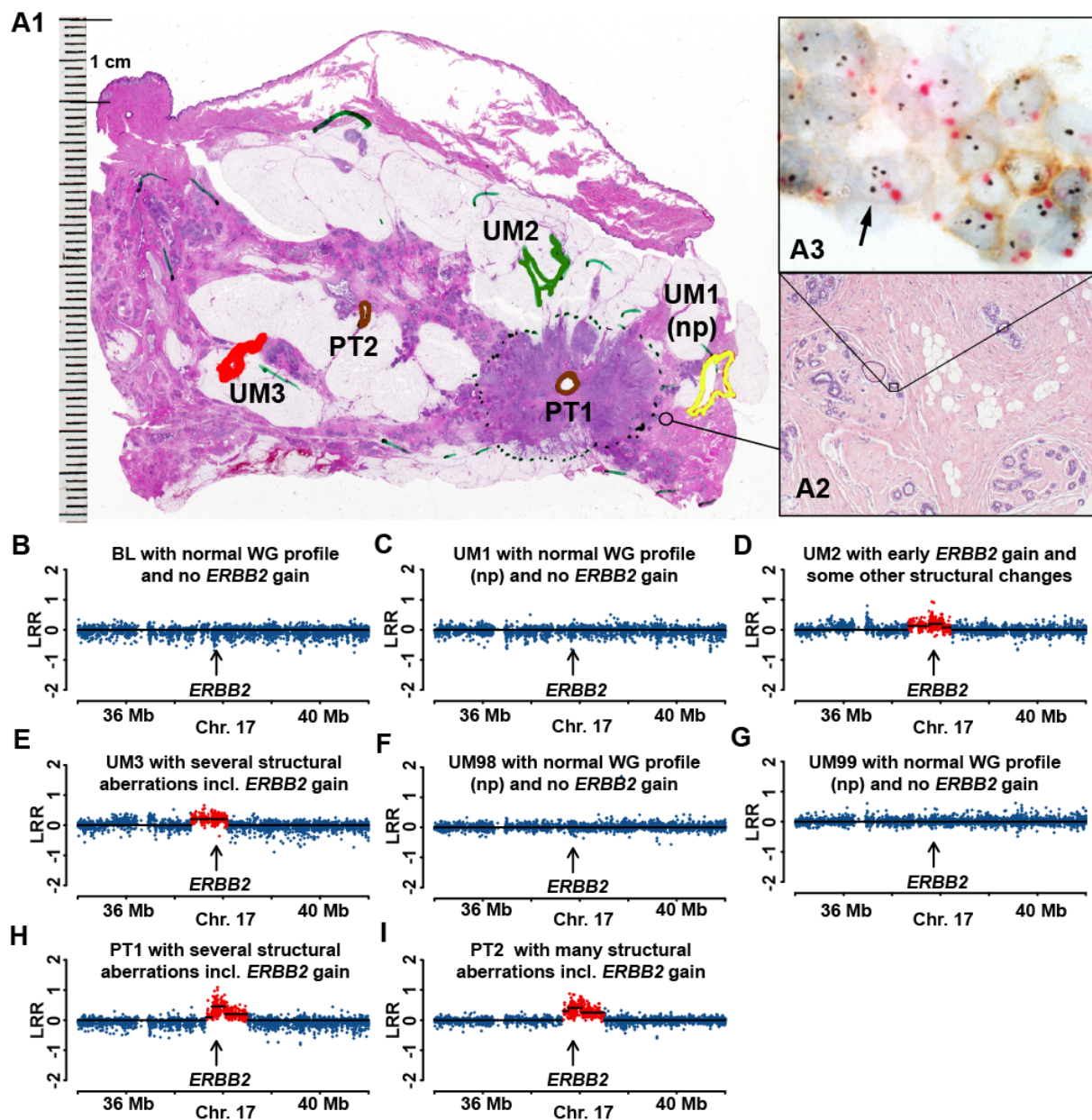
## Supplemental Figure 17



**Supplemental Figure 17.** Breast tissue in a sample VB from case 063JB shows increased gene copy number of the *FGFR1* gene on chromosome 8 and gain of the entire long arm of chromosome 1. Panels A and B show

representative images of breast parenchyma in hematoxylin and eosin stained frozen sections (approx. 5  $\mu\text{m}$ ) from specimen VB. This sample contained a mixture of areas with low-grade carcinoma *in situ* cells (panel A) and normal ducts (panel B). Panels C, D and E show the details of SNP-array for chromosome 1 and chromosome 8, the latter containing the *FGFR1* gene (red arrows) from analysis of blood (BL, normal control tissue), breast tissue from sample VB and primary tumor, respectively. As expected, sample BL show normal profile (panel C). Genomic segments in red in panels D and E were scored as abnormal in copy number (LRR track) and allelic ratio (BAF track). Sample VB shows a gain of *FGFR1* gene present in 30-50% of cells, as indicated by the BAF values deviating from the value of 0.5. In PT sample, the number of cells with a gain of the *FGFR1* gene is close to 100%. The total size of all aberrations present in VB specimen is 143.8 Mb, which is the lowest number in all studied samples containing cancer cells. Panels F and G show whole genome profiles for VB and PT samples. PT has multiple additional aberrations and also contains higher frequency of cells with the gain of the *FGFR1* gene and the gain of the entire long arm of chromosome 1. The position of the *FGFR1* gene is denoted by red arrows.

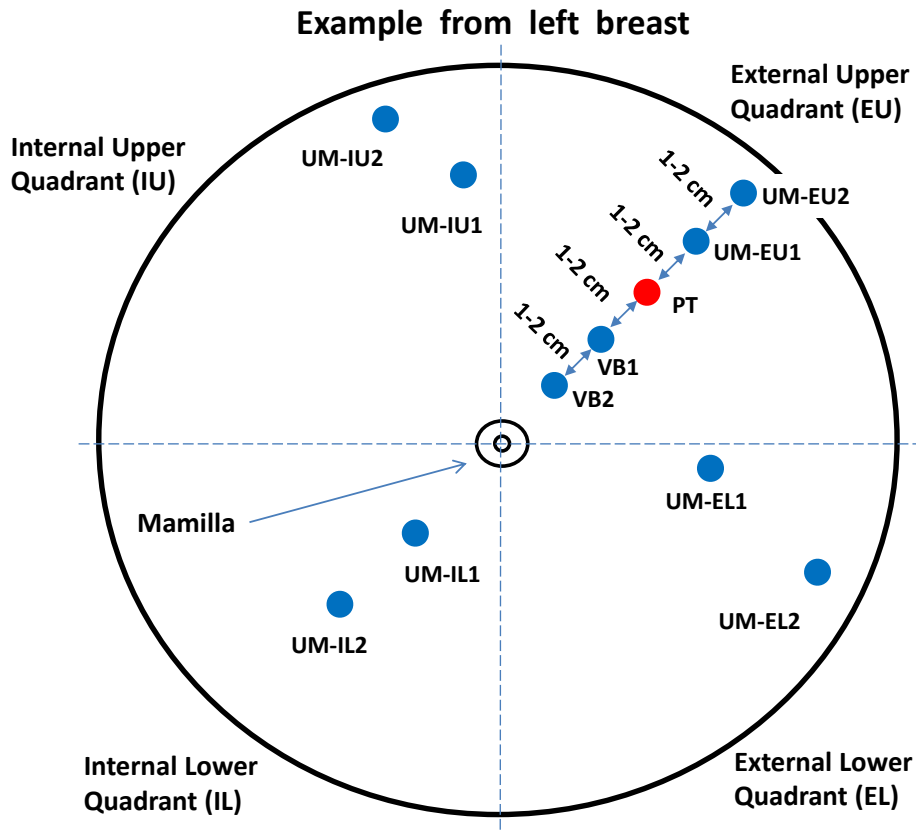
## Supplemental Figure 18



**Supplemental Figure 18.** Multimodal examination of pathology, gene copy number and gene expression for case MH047, with evidence of increased copy number and expression of the *ERBB2* gene in normal epithelial cells. Panel A1 shows a large-format histology slides of breast tissue from case MH047, with diagnosis of multifocal invasive ductal carcinoma (Luminal B, HER2+). Areas of tissue samples taken for DNA extraction, prior to formalin fixation of the tissue, are marked with colored thick lines. Positions of two primary tumors 1 and 2 (PT1 and PT2) are shown in brown. In panel A1, UM1, UM2 and UM3 are labelled in yellow, green, and red, respectively. (np) denotes normal genetic profiles (see also below panels B through I). A core of

paraffin-embedded breast tissue (thin-lined black circle) located between PT1 and UM1 was taken for separate analysis using tricolor HER2 Dual ISH DNA Probe Cocktail Assay (Roche) and the results are shown in panels A2 and A3. Panel A2 displays a histological image of normal breast, with cross-sections through terminal ductal lobular units (TDLUs). Black arrow in panel A3 points to a nucleus of a normal epithelial cell containing at least 3 copies of the *ERBB2* gene (black dots). Centromere of chromosome 17 is stained in red. Note a weak but clearly discernible immuno-histochemical staining of HER2 protein in the cell membrane of normal epithelial cells upon high magnification. Panels B through I show a segment of chromosome 17 containing the *ERBB2* gene in 8 samples from SNP-array. Blood (BL, normal control tissue), UM1, UM98 and UM99 samples show normal profiles (np) with no gain of the *ERBB2* gene. The remaining 4 samples were scored as containing increased copy number (red dots) for the *ERBB2* gene. The samples UM98 and UM99 are taken from parts of breast tissue as far away as possible from the segment (lobe) affected by breast cancer, in an area not visualized in panel A1. The total size of aberrations in UM samples is as follows: UM3, 12.4 Mb; and UM2, 74 Mb.

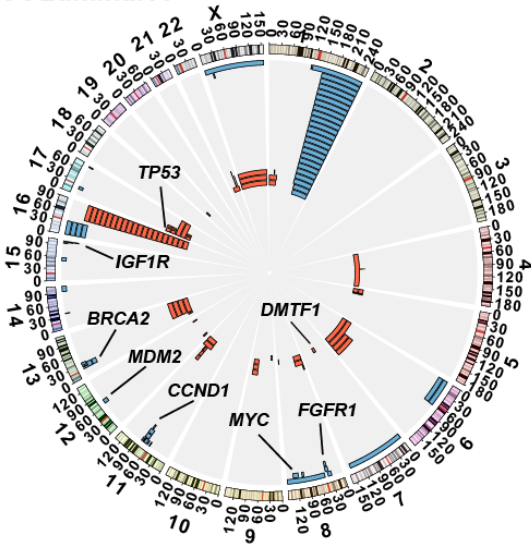
Supplemental Figure 19



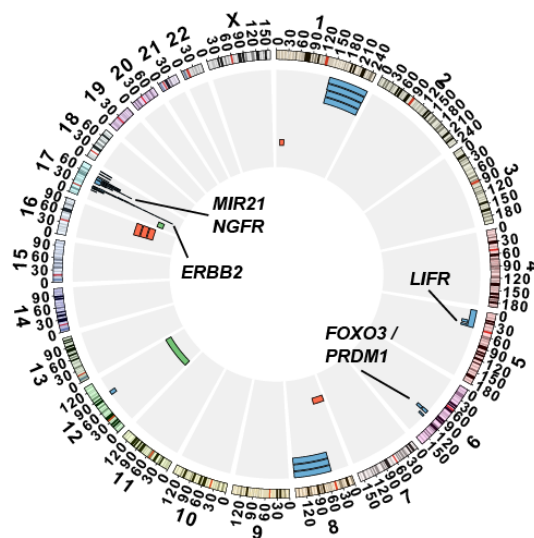
**Supplemental Figure 19.** A graphical outline of the protocol applied for collection of samples from Krakow and Gdansk centers. The black circle illustrates the breast, with division into four quadrants. UM = uninvolved margin; EU = external upper; IU = internal upper; IL = internal lower; EL = external lower. The primary tumor (PT) samples were often collected from the external upper quadrant of the breast, which is the frequent location of tumors. The distance between the macroscopically visible border of the primary tumor and the location of samples from the other quadrants (than the one where the tumor was located) was varying, due to often variable size of breast. The maximum distance was up to 15 cm.

# Supplemental figure 20

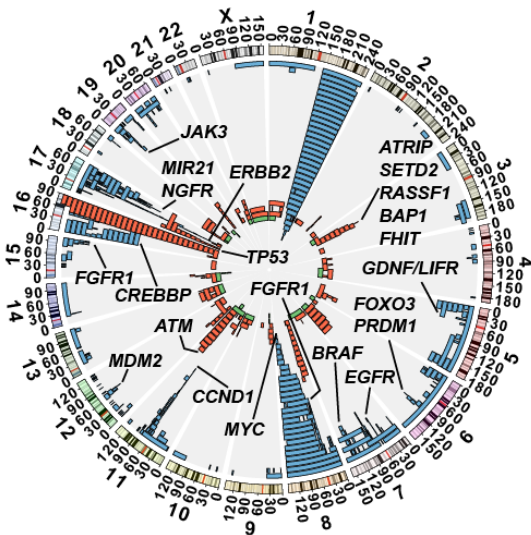
**A Luminal A**



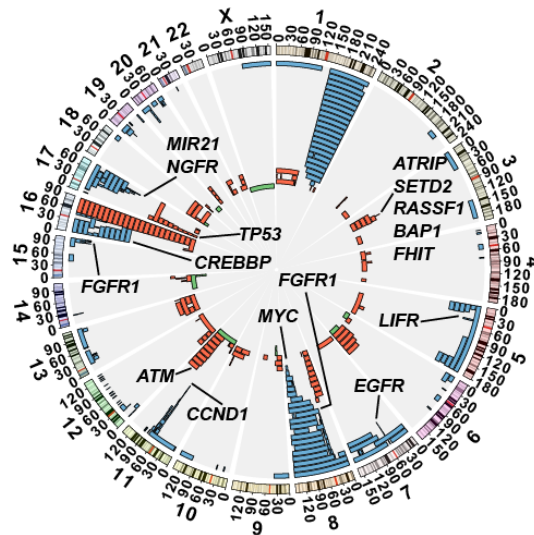
**B HER2 +**



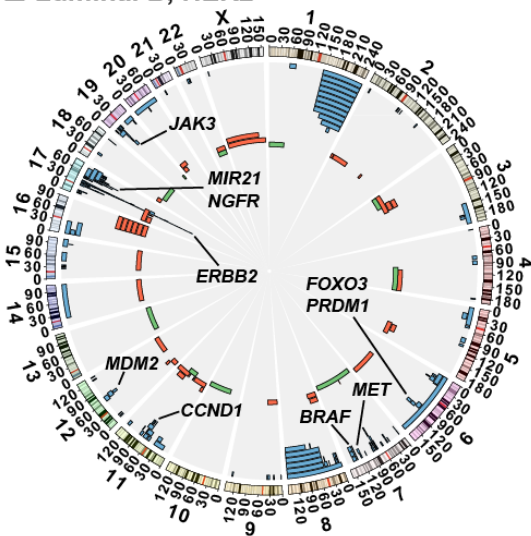
**C Luminal B**



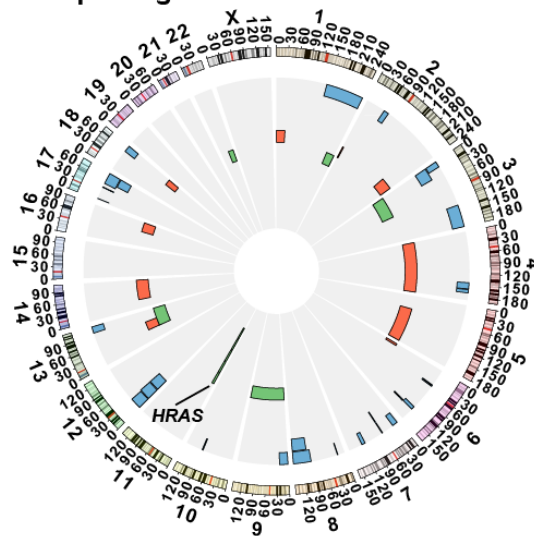
**D Luminal B, HER2 -**



**E Luminal B, HER2 +**



**F Triple negative**



**Supplemental Figure 20.** Representation of all size-determined aberrations detected in UM-samples from all cohorts, stratified by six molecular phenotypes of primary tumor. This phenotypic classification of tumors was performed according to St. Gallen 2011-standard (Goldhirsch et al. 2011). Three types of aberrations were detected using whole-genome Illumina SNP-array genotyping: gains=blue, deletions=red, CNNLOH/UPD=green, plotted using circos-plots (Krzywinski et al. 2009). The following numbers of UMs, subjects and three types of aberrations are included in each of the six plots:

- Panel A. Luminal A - 31 UMs from 21 subjects, 63 gains, 75 deletions and 2 CNNLOHs, a total of 140 variants;
- Panel B. HER2(+) - 16 UMs from 9 subjects, 56 gains, 5 deletions, 2 CNNLOHs, a total of 63 variants;
- Panel C. Luminal B - 90 UMs from 49 subjects, 438 gains, 178 deletions, and 21 CNNLOHs, a total of 637 variants;
- Panel D. Luminal B-HER2(-) - 55 UMs from 29 subjects, 223 gains, 137 deletions, 11 CNNLOHs, a total of 371 variants;
- Panel E. Luminal B, HER2(+) - 35 UMs from 20 subjects, 215 gains, 40 deletions, and 10 CNNLOHs, a total of 265 variants;
- Panel F. Triple negative - 16 UMs from 11 subjects, 30 gains, 10 deletions and 10 CNNLOHs, a total of 50 variants.

**Supplemental Table 1. Summary of clinical data and all genotyping experiments performed for 282 breast cancer cases, ordered by cohort.**

	Cohort	Case ID	Age at diagnosis	Tumor stage <sup>1</sup>	Histopathological diagnosis <sup>2</sup>	Tumor grade	Tumor focality <sup>3</sup>	Tumor molecular phenotype <sup>4</sup>	HER2 status (Lum. B) <sup>5</sup>	Number of controls genotyped <sup>6</sup>	Number of tumors genotyped	Number of UMs genotyped	Number of UMs with aberration
1	Krakow	001GZ	57	pT2N2	IDC	2	UF	Luminal B	-	1(B)	0	3	0
2	Krakow	002MP	58	pT2(m)N1	medullary ca.*	3	MF	Triple neg.*		1(B)	0	2	0
3	Krakow	003MC	65	pT2N1	ILC	2	UF	Luminal B	-	1(B)	0	5	0
4	Krakow	004JJ	71	pT2N1	IDC+DCIS	3	UF	Luminal B	-	1(B)	0	4	0
5	Krakow	005ZW	57	pT2N1	IDC	2	UF	Luminal B	-	1(B)	0	2	0
6	Krakow	006MK	51	pT2N1	IDC+DCIS	3	UF	Luminal B	-	1(S)	1	4	2
7	Krakow	007ETP	55	pT2N2	IDC	2	UF	Luminal A		1(B)	0	4	0
8	Krakow	008AG	46	pT2N1mi	IDC	2	UF	Luminal B	-	1(B)	0	4	0
9	Krakow	009SO	74	pT2N0	IDC	3	UF	HER2+		1(B)	0	4	0
10	Krakow	010LG	73	pT1cN0	IDC	3	UF	Luminal B	-	1(B)	0	3	0
11	Krakow	011BM	53	pT1cN2	IDC	2	UF	Luminal B	-	1(B)	1	2	1
12	Krakow	012MC	84	pT2N2	IDC+DCIS	3	UF	Luminal B	+	1(B)	1	6	1
13	Krakow	013WS	65	pT2N0	IDC+DCIS	3	MF	HER2+		1(B)	1	5	2
14	Krakow	014ZR	83	pT2N1	IDC+DCIS	3	UF	Luminal B	-	1(B)	0	3	0
15	Krakow	015SK	72	pT1cN0	IDC (mucinous comp.*)	3	UF	Luminal B	-	1(B)	0	5	0
16	Krakow	016JS	72	pT3N0	IDC	3	UF	Triple neg.*		1(B)	1	4	1
17	Krakow	017KM	82	pT1cN2	IDC+DCIS	2	UF	Luminal B	-	1(S)	1	5	5
18	Krakow	018MS	51	pT2N2	IDC	3	MF	HER2+		1(B)	0	5	0
19	Krakow	019ZB	63	pT2N2	IDC+DCIS	3	UF	HER2+		1(B)	0	4	0
20	Krakow	020HK	68	pT2N1	IDC	2	UF	Luminal B	-	1(B)	0	3	0
21	Krakow	021MB	64	pT4bN2	ILC	2	UF	Luminal B	+	1(B)	1	5	2
22	Krakow	022ZT	45	pT1cN1	IDC	3	UF	Luminal B	+	1(B)	0	4	0
23	Krakow	023GC	56	pT2(m)N3	IDC	3	MF	Luminal B	+	1(B)	0	3	1
24	Krakow	024MZ	35	pT2N0	IDC+DCIS	3	UF	Luminal B	-	1(B)	1	5	1
25	Krakow	025JT	56	pT2N1	IDC+DCIS	3	UF	Luminal B	-	1(B)	1	5	1
26	Krakow	026MS	48	pT2N0	IDC	3	UF	Triple neg.*		1(B)	1	5	1
27	Krakow	027MW	41	pT2N0	IDC+DCIS	2	UF	Luminal B	-	1(B)	0	4	0
28	Krakow	028BM	66	pT1cN0	IDC+DCIS	3	UF	Triple neg.*		1(B)	0	5	0
29	Krakow	029LN	81	pT2N0	ILC	2	UF	Luminal B	-	1(B)	0	4	0
30	Krakow	030SK	61	ypT3N2	IDC	2	MF	Luminal B	-	1(B)	0	5	0
31	Krakow	031EJ	46	pT1cN2	IDC+DCIS	2	UF	Luminal B	-	1(B)	0	4	0
32	Krakow	032AG	45	pT2N3	IDC	3	UF	Luminal B	+	1(B)	0	4	0
33	Krakow	033DK	42	pT2N3	IDC+DCIS	3	UF	Luminal B	+	1(B)	0	5	0
34	Krakow	034IG	75	ypT2N0	IDC	3	UF	Luminal B	+	1(B)	0	4	0
35	Krakow	035TG	74	pT2N0	IDC+DCIS	3	UF	Triple neg.*		1(B)	0	4	0
36	Krakow	036CS	57	pT2N0	IDC+DCIS apocrine	3	UF	HER2+		1(B)	0	3	0
37	Krakow	037MC	58	pT2N1	ILC+LCIS	2	UF	Luminal A		1(B)	1	3	2
38	Krakow	038ALZ	58	pT2N2	IDC (apocrine comp.*)	3	UF	HER2+		1(B)	0	5	0
39	Krakow	039BW	62	pT2N0	IDC	3	UF	Triple neg.*		1(B)	1	4	0
40	Krakow	040HM	72	pT2N1mi	IDC	3	UF	HER2+		1(B)	0	5	0
41	Krakow	041JS	48	pT1cN3	IDC	3	UF	Luminal B	-	1(B)	0	5	0
42	Krakow	042JL	78	pT2N3	IDC+DCIS	3	UF	Triple neg.*		1(B)	0	5	0
43	Krakow	043WB	79	pT2N0	ILC	2	UF	Luminal A		1(B)	1	5	1
44	Krakow	044JD	74	pT1cN1	IDC	2	UF	Luminal B	-	1(B)	0	4	1
45	Krakow	045EK	54	pT2N1	IDC + IPC	3	UF	Triple neg.*		1(B)	0	5	0
46	Krakow	046MU	66	pT1cN0	IDC+DCIS	2	UF	Luminal A		1(B)	0	5	0
47	Krakow	047MS	68	pT1cN0	TC+ICC	1	UF	Triple neg.*		1(B)	0	5	0
48	Krakow	048EB	71	pT2N0	IDC	3	UF	Luminal B	-	1(B)	0	5	0
49	Krakow	049ASZ	61	pT1cN1	ILC+LCIS	2	UF	Luminal A		1(B)	1	5	2
50	Krakow	050RW	50	pT2(m?)N3	IDC	3	MF	HER2+		1(B)	0	5	0
51	Krakow	051AZ	82	pT1cN2	IDC (apocrine comp.*)	3	UF	Triple neg.*		1(B)	0	6	0
52	Krakow	052JW	42	pT2(m)N2	IDC	3	MF	Triple neg.*		1(B)	0	4	0

53	Krakow	053KS	57	pT1miN0	DCIS + Paget's ca.*	DCIS	DCIS MF	Unclassif.*		1(B)	1	5	1
54	Krakow	054MJ	55	pT1cN0	IDC	3	UF	Luminal B	-	1(B)	1	2	1
55	Krakow	055GG	55	pT2N0	ILC	2	UF	Luminal B	-	1(B)	0	5	0
56	Krakow	056AKP	78	pT2N0	IDC	3	UF	Luminal B	+	1(B)	0	5	0
57	Krakow	057GS	50	pT2N1	IDC+DCIS	2	UF	Luminal B	+	1(B)	0	5	0
58	Krakow	058ZA	61	pT2N0	IDC	3	UF	Luminal B	-	1(B)	0	5	0
59	Krakow	059HS	59	pT2N0	IDC apocrine	3	UF	HER2+		1(B)	0	4	0
60	Krakow	060HP	63	pT2(m)N0	IC (IDC comp.*)	3	MF	Luminal B	-	1(B)	0	5	0
61	Krakow	061AS	75	pT2N0(ITC)	ILC atypical	3	UF	HER2+		1(B)	1	5	1
62	Krakow	062BI	55	pT1cN1	IDC+DCIS	3	UF	Luminal A		1(B)	1	4	1
63	Krakow	063JB	67	pT1c(m)N2	IDC	2	MF	Luminal B	-	1(B)	1	5	2
64	Krakow	064KK	71	pT2(m)N1	IDC	3	MF	Luminal B	-	1(B)	0	5	0
65	Krakow	065AS	82	pT2N1	metaplastic (squamous) ca.*	3	UF	Triple neg.*		1(B)	1	3	1
66	Krakow	066JD	59	pT2N0	IDC	2	UF	Luminal A		1(B)	0	5	0
67	Krakow	067JB	68	pT2N1	IDC (ICC comp.*)	2	UF	Luminal A		1(B)	0	4	0
68	Krakow	068AP	78	pT2N0	IDC	2	UF	Luminal A		1(B)	0	5	0
69	Krakow	069EKJ	74	pT2N0	IDC+DCIS	3	UF	Luminal A		1(B)	0	5	0
70	Krakow	070ZNK	53	pT2N2	IDC	3	UF	Triple neg.*		1(B)	1	2	1
71	Krakow	071ZB	66	pT2N1	IDC	3	UF	Triple neg.*		1(B)	1	5	1
72	Krakow	072KS	63	pT1cN0	ILC	2	UF	Luminal A		1(B)	1	5	0
73	Krakow	073TS	58	pT2N1	IDC	2	UF	Luminal B	-	1(B)	0	5	0
74	Krakow	074DP	49	pT1cN1	IDC	2	UF	Luminal B	-	1(B)	0	5	0
75	Krakow	075JS	65	pT3(m)N2	IDC	3	MF	Luminal B	-	1(B)	1	4	1
76	Krakow	076MW	51	pT2N2	mixed ca.* (mucinous + micropapillary + IDC)	3	UF	Luminal A		1(B)	0	5	0
77	Krakow	077EP	61	pT2N2	IDC+DCIS	2	UF	Luminal B	+	1(B)	1	2	2
78	Krakow	078AW	63	pT2N2	IDC+DCIS	2	UF	Luminal B	+	1(B)	1	5	1
79	Krakow	079KN	81	pT2N2	invasive ca. (papillary comp.*)	3	UF	Luminal B	-	1(B)	0	4	0
80	Krakow	080SJ	85	pT1cN2	IDC	2	UF	Luminal A		1(B)	0	5	0
81	Krakow	081BS	48	pT2N2	IDC+DCIS	3	UF	Luminal B	-	1(B)	1	5	3
82	Krakow	082HM	53	pT2N0	IDC	3	UF	Triple neg.*		1(B)	0	4	0
83	Krakow	083JSZ	69	pT2N0	IDC+DCIS	3	UF	Triple neg.*		1(B)	0	3	0
84	Krakow	084WP	74	pT2N2	IDC+IPC	3	UF	Luminal B	-	1(B)	0	5	0
85	Krakow	085AS	74	pT2N2	IDC+DCIS	2	UF	Luminal B	-	1(B)	1	4	2
86	Krakow	086AFT	71	pT2N1	IDC+DCIS	3	UF	Luminal B	+	1(B)	1	5	1
87	Krakow	087EW	74	pT2N3	IDC+DCIS	2	UF	Luminal B	-	1(B)	0	5	0
88	Krakow	088AW	48	pT2N1	IDC	2	UF	Luminal B	-	1(B)	0	5	0
89	Krakow	089SD	60	pT2N0	IDC apocrine+DCIS	3	UF	Triple neg.*		1(B)	1	6	2
90	Krakow	090MP	35	pT2N2	IDC+DCIS	2	UF	Luminal B	-	1(B)	0	5	0
91	Krakow	091MB	58	pT2N1	IDC	3	UF	Luminal B	-	1(B)	0	4	0
92	Krakow	092SP	81	pT2N1	IDC+DCIS	2	UF	Luminal B	-	1(B)	1	5	0
93	Krakow	093AZ	71	pT1cN1	IDC+DCIS	2	UF	Luminal B	+	1(B)	0	4	0
94	Krakow	094MSZ	73	pT1cN2	IDC	2	UF	Unclassif.*		1(B)	0	4	0
95	Krakow	095ESZ	49	pT1bN2	ILC+LCIS	2	UF	HER2+		1(B)	1	5	2
96	Krakow	096MSZ	55	pT2N1	IDC+DCIS	2	UF	Luminal B	-	1(B)	0	5	0
97	Krakow	097MM	62	pT2N0	ILC	2	UF	Luminal A		1(B)	0	4	0
98	Krakow	098WC	69	pT2N1	IDC+DCIS	3	UF	Luminal B	-	1(B)	1	5	2
99	Krakow	099OLZ	63	pT2N0	IDC+DCIS	3	UF	Triple neg.*		1(B)	0	5	1
100	Krakow	100AW	60	pT2(m)N0	IDC+ICC+IPC	3	MF	Luminal B	-	1(B)	1	5	3
101	Krakow	101ZM	75	pT1cN1	IDC	2	UF	Luminal B	-	1(B)	0	5	0
102	Krakow	123HS	66	pT2N0	IDC+DCIS	2	UF	Luminal B	-	1(S)	1	6	0
103	Krakow	124AA	56	pT1c(m)N3	IDC (apocrine comp.*)+ DCIS	3	MF	HER2+		1(B)	0	6	0

104	Krakow	125KL	67	pT2N0	ILC	2	UF	Luminal B	-	1(B)	0	6	0
105	Krakow	126AS	85	pT4bN1	IDC	2	UF	HER2+		1(B)	0	5	0
106	Krakow	127ZR	54	pT2N2	IDC	3	UF	HER2+		1(B)	0	5	0
107	Krakow	128WS	62	pT2N0	IDC	3	UF	Luminal B	+	1(B)	0	6	0
108	Krakow	129EB	69	pT2N0	ILC	2	MF	Luminal B	-	1(S)	1	5	1
109	Krakow	130JT	50	pT2N2	IDC+DCIS	3	UF	Luminal B	+	1(S)	1	6	2
110	Krakow	131SD	82	pT1cN0	mucinous ca.*	2	UF	Luminal A		1(S)	1	5	1
111	Krakow	132EM	47	pT2N2	IDC	2	UF	Luminal B	-	1(B)	0	4	0
112	Krakow	133ML	34	pT1cN2	IDC+DCIS	2	UF	Luminal B	-	1(S)	1	6	3
113	Krakow	134GJ	75	pT1cN0	IDC	3	UF	Luminal A		1(B)	0	6	0
114	Krakow	135LS	74	pT1cN1	IDC	2	UF	Luminal B	+	1(B)	0	6	0
115	Krakow	136BS	77	pT2N1	IDC	2	UF	Luminal A		1(B)	0	6	0
116	Krakow	137WK	87	Unclassif.*	IDC	2	UF	Luminal A		1(B)	0	3	0
117	Krakow	138BM	35	pT1cN0	IDC+DCIS	3	UF	Luminal B	-	1(S)	1	6	1
118	Krakow	139MD	48	pT2N1	IDC+DCIS	2	UF	Luminal B	-	1(S)	1	6	2
119	Krakow	140MF	31	pT2N1	medullary ca.*	3	UF	Triple neg.*		1(B)	0	6	0
120	Krakow	141BB	58	pT2N1	ILC	2	UF	Luminal B	-	1(S)	1	6	3
121	Krakow	142AK	54	pT2Nx	IDC + DCIS + Paget's ca.*	3	UF	Luminal B	+	1(S)	1	6	1
122	Krakow	143DMG	46	pT2N0	IDC+ILC+DCIS+ LCIS	2	UF	Luminal B	-	1(S)	1	6	2
123	Krakow	144BW	57	pT2(m)N2	IDC+DCIS	3	MF	Luminal B	-	1(B)	0	6	0
124	Krakow	145MJ	61	pT1cN1	IDC	2	UF	Luminal A		1(B)	0	6	0
125	Krakow	AD171	76	pT2N1	IDC	3	UF	Luminal B	-	1(B)	1	9	0
126	Krakow	AL148	55	pT2N3	IDC	3	UF	Triple neg.*		1(B)	1	12	0
127	Krakow	DM153	44	pT2N1	IDC	3	UF	Triple neg.*		1(B)	1	10	0
128	Krakow	EG163	45	pT2(m)N3	IDC+DCIS	3	MF	HER2+		1(B)	1	10	3
129	Krakow	EW155	67	pT1cN2	IDC+DCIS	3	UF	Luminal B	-	1(B)	1	14	2
130	Krakow	GC146	70	pT1cN0	IDC+DCIS	2	UF	Luminal A		1(S)	1	12	0
131	Krakow	GC147	70	pT2N2	IDC	3	UF	Luminal A		1(S)	1	10	3
132	Krakow	GS166	56	pT3N1	IDC	3	UF	Triple neg.*		1(B)	1	10	2
133	Krakow	HZK162	75	pT2N1	IDC	1	UF	Luminal B	-	1(B)	1	9	1
134	Krakow	JM154	74	pT2N1	IDC+DCIS	3	UF	Luminal B	-	1(B)	1	8	0
135	Krakow	JP149	44	pT2N1	IDC	3	UF	Triple neg.*		1(B)	1	12	1
136	Krakow	JW167	53	pT2N1	IDC	2	UF	Luminal B	+	1(B)	1	8	0
137	Krakow	KK151	54	pT1cN2	IDC+IPC+DCIS	3	UF	Luminal B	+	1(B)	1	12	4
138	Krakow	KM159	84	pT1cN2	IDC	2	UF	Luminal A		1(B)	1	9	1
139	Krakow	KS150	35	pT3N1	IDC	3	UF	Luminal B	-	1(B)	1	8	1
140	Krakow	KS165	81	pT2N2	IDC+DCIS	2	UF	Luminal A		1(B)	1	10	0
141	Krakow	MP172	80	pT2N0	IDC	2	UF	Unclassif.*		1(B)	1	12	0
142	Krakow	MS168	71	pT1cN1mi	IPC	2	UF	Luminal B	-	1(B)	1	12	1
143	Krakow	MW158	39	pT2N3	IDC	3	UF	Luminal B	-	1(B)	1	9	6
144	Krakow	SD164	47	pT2N3	IDC	2	UF	Luminal B	-	1(B)	1	12	2
145	Krakow	TP169	62	pT1cN1	IDC	3	UF	HER2+		1(B)	1	12	1
146	Krakow	ZL152	57	pT2N0	IDC	2	UF	Luminal B	+	1(B)	1	12	1
147	Falun	AB007	54	pT1cN0	IDC	2	MF	HER2+		1(S)	2	4	0
148	Falun	ACV037	64	pT2N1a	IDC	2	MF	Luminal B	+	1(S)	1	4	1
149	Falun	AE031	49	pT3N2a	IDC	2	MF	Luminal A		1(S)	2	5	1
150	Falun	AH028	70	pT1cN0	ILC	2	MF	Luminal B	-	1(B)	3	6	2
151	Falun	AKK034	62	pT1bN1a	IDC	1	MF	Luminal A		1(S)	2	6	0
152	Falun	AL002	49	pT3N2a	IDC	3	MF	Luminal B	+	1(S)	3	4	3
153	Falun	AW020	36	pT3N1a	IDC	2	MF	Luminal B	+	1(B)	3	8	5
154	Falun	BD038	53	pT1cN0	IDC	2	MF	Luminal A		1(S)	2	4	3
155	Falun	BG021	64	pT1cN0	IDC	2	UF	Luminal A		1(B)	2	4	0
156	Falun	BL049	63	pT1bN0	IDC	1	UF	Luminal A		1(B)	1	4	0
157	Falun	BMF005	55	pT2N1a	IDC	3	MF	HER2+		1(S)	2	5	2
158	Falun	BMK015	53	pT3N1a	IDC	2	MF	Luminal A		1(S)	2	5	1
159	Falun	BSP017	71	pT1cN1a	mucinous ca.*	2	MF	Luminal B	+	1(S)	2	5	0
160	Falun	CG010	38	n.a.	DCIS	3	MF	Unclassif.*		1(S)	1	3	1
161	Falun	CH048	60	pT1bN0	IDC	1	UF	Luminal A		1(B)	1	4	0
162	Falun	CT055	54	pT1cN0	IDC	1	MF	Luminal B	-	1(B)	1	5	0

163	Falun	DO044	52	pT2N2a	IDC	3	MF	HER2+	1(B)	2	6	0	
164	Falun	ED027	80	pT2N0	ILC	3	MF	Luminal A	1(B)	2	5	0	
165	Falun	EF046	69	pT1cN0	IDC	2	UF	Luminal A	1(B)	1	4	0	
166	Falun	EN039	60	pT2N1a	IDC	2	MF	Luminal B	-	1(S)	2	6	0
167	Falun	ER033	58	pT2N0	IDC	3	UF	Triple neg.*	1(S)	1	4	0	
168	Falun	GGB040	63	pT3N1a	IDC	2	MF	Luminal B	-	1(S)	3	6	4
169	Falun	GS011	74	pT1cN0	IDC	2	UF	Luminal B	-	1(S)	1	4	1
170	Falun	HB054	47	pT1bN1a	ILC	2	MF	Luminal A	1(B)	3	6	0	
171	Falun	HL057	71	pT2N0	IDC	2	MF	Luminal A	1(S)	3	6	0	
172	Falun	HS006	49	pT2N0	ILC	2	MF	Luminal A	1(B)	1	1	1	
173	Falun	ILN025	70	pT2N3a	IDC	2	MF	Luminal A	1(B)	2	3	0	
174	Falun	ILS024	73	pT1cN0	ILC	2	MF	Luminal A	1(B)	2	4	0	
175	Falun	IMH013	73	pT1bN0	TLC	2	MF	Luminal A	1(B)	2	4	1	
176	Falun	IP008	41	pT2N2a	IDC	3	MF	Luminal A	1(S)	1	3	1	
177	Falun	KVS035	67	pT1bN0	IDC	1	MF	Luminal A	1(S)	2	5	0	
178	Falun	LEB004	48	pT2N3a	IDC	3	MF	Triple neg.*	1(S)	2	5	0	
179	Falun	LF042	50	pT1cN0	ILC	2	MF	Luminal A	1(B)	2	6	1	
180	Falun	LH045	85	pT3N1a	ILC	2	MF	Luminal A	1(B)	2	5	3	
181	Falun	LK003	64	pT2N1a	IDC	2	MF	Luminal A	1(S)	2	4	1	
182	Falun	LM022	59	pT2N0	IDC	2	MF	Luminal A	1(B)	2	5	0	
183	Falun	LR050	50	pT1bN0	IDC	1	UF	Luminal A	1(B)	1	4	0	
184	Falun	MA018	84	pT4bN2a	IDC	3	MF	HER2+	1(S)	2	5	3	
185	Falun	MAL026	94	pT1cN1c	IDC	1	MF	Luminal A	1(S)	2	4	0	
186	Falun	MB032	56	pT2N3a	IDC	2	MF	Luminal B	-	1(S)	4	5	2
187	Falun	MD041	59	pT1cN1a	IDC	1	UF	Luminal B	-	1(B)	1	3	0
188	Falun	MD052	63	pT1cN0	ILC pleomorph	3	MF	Luminal B	-	1(B)	1	4	2
189	Falun	ME029	58	pT1cN1a	IDC	2	MF	Luminal B	-	1(B)	2	4	1
190	Falun	MH016	53	pT3N1a	IDC	2	MF	Luminal B	+	1(S)	2	6	1
191	Falun	MH047	44	pT2N1a	IDC	3	UF	Luminal B	+	1(B)	2	5	2
192	Falun	MJQ051	45	pT3N1a	IDC	3	UF	Triple neg.*	1(B)	1	4	0	
193	Falun	ML012	49	pT3N0	ILC	2	MF	Luminal A	1(S)	1	4	2	
194	Falun	MN036	50	pT1cN1a	IDC	3	MF	Luminal B	+	1(S)	3	8	5
195	Falun	NHB053	45	pT1cN0	IDC	1	MF	Luminal A	1(B)	2	5	0	
196	Falun	RJ019	57	pT1bN2a	TLC	2	MF	Luminal A	1(B)	2	3	0	
197	Falun	SK056	49	pT2N0	IDC	3	MF	Triple neg.*	1(B)	3	5	2	
198	Falun	SW030	75	pT1cN0	ILC	2	MF	Luminal A	1(S)	2	4	0	
199	Falun	UBM043	63	pT1cN0	IDC	1	UF	Luminal A	1(B)	1	4	0	
200	Falun	UV023	49	pT2N2a	IDC	2	MF	Luminal A	1(B)	2	6	2	
201	Gdansk	BK008	48	pT2N1Mx	IDC	2	UF	Luminal B	+	1(S)	1	3	1
202	Gdansk	BM003	59	pT3N0Mx	metaplastic ca.*	3	UF	Unclassif.*	1(S)	1	3	0	
203	Gdansk	EJ001	80	pT4N3Mx	ILC	2	UF	Triple neg.*	1(B)	1	5	5	
204	Gdansk	GI004	62	pT2N0Mx	ILC	2	MF	Luminal A	1(S)	1	3	0	
205	Gdansk	JE009	52	pT2N0Mx	IDC	3	UF	Luminal B	+	1(S)	1	2	0
206	Gdansk	MD006	49	pT2N2Mx	IDC	3	MF	HER2+	1(S)	1	3	2	
207	Gdansk	PA002	50	pT4aN1Mx	IDC	2	UF	Luminal B	-	1(B)	1	4	0
208	Gdansk	PD005	57	pT2N2Mx	IDC	3	UF	HER2+	1(S)	1	3	0	
209	Gdansk	RK010	54	pTxN0M1	Unclassif.*	n.a	Unclassif.*	Luminal B	+	1(S)	1	2	0
210	Gdansk	WK007	68	pT2N0Mx	IDC	2	UF	Luminal B	-	1(S)	1	2	0
211	Bydgoszcz	BE89	40	ypT2N2a	Unclassif.*	3	UF	HER2+	1(B)	0	1	0	
212	Bydgoszcz	BH81	70	pT1cN0	ILC	2	UF	Luminal B	-	1(B)	0	1	0
213	Bydgoszcz	BK152	55	pT2 N1a	ILC	2	MF	Luminal B	+	1(B)	1	1	1
214	Bydgoszcz	BK9	n.a	n.a	n.a	n.a	n.a	n.a	1(B)	0	1	1	
215	Bydgoszcz	BL87	67	pT1cN0	IDC	2	UF	Luminal A	1(B)	0	1	0	
216	Bydgoszcz	BM50	59	pT2N2a	IDC	3	UF	HER2+	1(B)	0	1	0	
217	Bydgoszcz	BU97	46	pT2N0	IDC	2	UF	Triple neg.*	1(B)	1	1	1	
218	Bydgoszcz	CB110	66	pT1cN0	IDC	2	UF	Luminal B	-	1(B)	0	1	0
219	Bydgoszcz	CJ112	55	pT2N0	medullary ca.*	3	UF	Triple neg.*	1(B)	1	1	1	
220	Bydgoszcz	CM155	61	pT2N2a	IDC	2	UF	Luminal B	-	1(B)	0	1	0
221	Bydgoszcz	DA83	53	pT1cN0	IDC	2	UF	Luminal A	1(B)	0	1	0	
222	Bydgoszcz	DE108	76	pT1cN0	ILC	2	UF	Luminal A	1(B)	0	1	0	
223	Bydgoszcz	DE137	52	pT1cN1a	IDC	2	UF	Luminal A	1(B)	0	1	0	

224	Bydgoszcz	DE22	48	pT2N1a	ILC alveolar type	2	UF	Luminal B	-	1(B)	1	1	0
225	Bydgoszcz	DH74	40	pT2N0	IDC	3	UF	Triple neg.*		1(B)	1	1	1
226	Bydgoszcz	DM138	46	pT2N2a	IDC	2	UF	Luminal A		1(B)	1	1	1
227	Bydgoszcz	FK12	71	pT1cN0	IDC	2	UF	Triple neg.*		1(B)	0	1	0
228	Bydgoszcz	GK1	63	pT1cN0	ILC	2	UF	Luminal A		1(B)	0	1	0
229	Bydgoszcz	GW39	46	pT1cN1a	IDC	2	UF	Luminal A		1(B)	0	1	0
230	Bydgoszcz	GW55	56	pT1cN0	IDC	2	UF	Luminal B	-	1(B)	0	1	0
231	Bydgoszcz	HW82	55	pT2N2a	IDC	2	UF	Triple neg.*		1(B)	0	1	0
232	Bydgoszcz	JB11	57	pT2N0	mucinous ca.*	1	MF	Triple neg.*		1(B)	0	1	0
233	Bydgoszcz	JD67	40	pT2N3a	ILC alveolar type	2	UF	Luminal B	-	1(B)	0	1	1
234	Bydgoszcz	JJ144	77	pT2N0	IDC	2	UF	Triple neg.*		1(B)	0	1	0
235	Bydgoszcz	JM43	75	pT2 N1a	IDC	2	UF	HER2+		1(B)	1	1	0
236	Bydgoszcz	JU32	62	pT2N1a	IDC	2	UF	HER2+		1(B)	1	1	1
237	Bydgoszcz	KA15	70	pT2N3a	IDC	2	UF	Luminal B	-	1(B)	0	1	0
238	Bydgoszcz	KB132	64	pT2N2a	IDC	3	MF	Luminal B	-	1(B)	1	1	1
239	Bydgoszcz	KB80	47	pT1cN0	IDC	2	UF	Luminal A		1(B)	0	1	0
240	Bydgoszcz	KE127	44	ypT2N3a	Unclassif.*	3	UF	HER2+		1(B)	0	1	0
241	Bydgoszcz	KE53	60	pT2N0	IDC	2	UF	Triple neg.*		1(B)	0	1	0
242	Bydgoszcz	KG13	72	pT2N2a	ILC	2	UF	Luminal B	+	1(B)	2	1	0
243	Bydgoszcz	KH95	73	pT2N1a	IDC	2	UF	Luminal A		1(B)	0	1	0
244	Bydgoszcz	KJ142	75	pT4N0	ILC	2	UF	HER2+		1(B)	0	2	0
245	Bydgoszcz	KK123	62	pT2N0	IDC	2	UF	Luminal A		1(B)	1	1	1
246	Bydgoszcz	KM136	46	pT1cN1a	ILC	2	MF	Luminal B	-	1(B)	0	1	0
247	Bydgoszcz	KM143	44	pT1bN0	ILC	2	UF	Unclassif.*		1(B)	0	1	0
248	Bydgoszcz	KM19	48	pT1cN0	ILC	2	UF	Luminal B	+	1(B)	0	1	0
249	Bydgoszcz	KS141	33	pT2N0	IDC	3	UF	Triple neg.*		1(B)	1	1	1
250	Bydgoszcz	KU25	51	pT1cN0	IDC	2	UF	Luminal A		1(B)	1	1	0
251	Bydgoszcz	KZ54	52	pT2N0	IDC	2	UF	Luminal B	+	1(B)	0	1	1
252	Bydgoszcz	MB101	60	pT1cN0	IDC	2	UF	Luminal A		1(B)	0	1	0
253	Bydgoszcz	MC109	47	pT1cN2a	IDC	2	UF	Unclassif.*		1(B)	0	1	0
254	Bydgoszcz	MD106	52	pT1cN0	IDC	2	MF	Luminal A		1(B)	0	1	0
255	Bydgoszcz	MD86	51	pT2N0	IDC	2	UF	Luminal A		1(B)	0	1	0
256	Bydgoszcz	ME114	56	pT2N0	medullary ca.*	3	UF	Luminal B	+	1(B)	1	1	1
257	Bydgoszcz	MG124	58	pT1cN0	IDC	2	UF	Triple neg.*		1(B)	0	1	0
258	Bydgoszcz	MK120	57	pT2N0	IDC	2	UF	Luminal A		1(B)	1	1	1
259	Bydgoszcz	ML36	60	pT2 N2a	IDC	2	UF	Luminal B	-	1(B)	2	3	3
260	Bydgoszcz	MM115	64	pT2N0	IPC	3	MF	Luminal A		1(B)	0	1	0
261	Bydgoszcz	MM69	27	pT1cN0	IDC	2	MF	Luminal B	-	1(B)	2	1	0
262	Bydgoszcz	MU154	70	pT1cN2a	IDC	2	UF	Luminal B	-	1(B)	1	1	0
263	Bydgoszcz	NA71	77	pT2N1a	IDC	2	UF	Luminal B	-	1(B)	0	1	0
264	Bydgoszcz	NJ111	57	pT2N0	IDC	2	UF	Triple neg.*		1(B)	0	1	0
265	Bydgoszcz	NM48	66	pT2N0	IDC	2	UF	Luminal B	+	1(B)	2	1	1
266	Bydgoszcz	OB125	69	pT1cN0	ILC	2	UF	Luminal A		1(B)	0	1	0
267	Bydgoszcz	OG93	79	pT2N2a	ILC	2	UF	Luminal A		1(B)	0	1	0
268	Bydgoszcz	OH113	47	pT2 N1a	IDC	3	UF	Luminal B	-	1(B)	0	1	1
269	Bydgoszcz	PE103	62	pT1cN0	IDC	2	UF	Luminal A		1(B)	0	1	0
270	Bydgoszcz	PE129	37	pT2N0	IDC	2	UF	Luminal B	-	1(B)	1	1	0
271	Bydgoszcz	PF27	68	pT2N3a	ILC	2	UF	Luminal B	-	1(B)	2	1	0
272	Bydgoszcz	PI33	79	pT2 N2a	ICD	2	UF	Luminal B	-	1(B)	1	1	1
273	Bydgoszcz	PJ121	61	pT2N1a	ILC	2	UF	Luminal B	-	1(B)	0	1	0
274	Bydgoszcz	PJ133	67	pT2N1a	IDC	2	UF	Luminal A		1(B)	0	1	0
275	Bydgoszcz	PK6	68	pT2N2a	IDC	3	UF	Luminal B	-	1(B)	1	1	0
276	Bydgoszcz	PM102	65	pT2 N1a	IDC	2	UF	Triple neg.*		1(B)	1	1	1
277	Bydgoszcz	RA35	33	ypT3N3a	Unclassif.*	3	UF	Triple neg.*		1(B)	0	1	0
278	Bydgoszcz	RB84	73	pT2N0	ILC	2	UF	Unclassif.*		1(B)	0	1	0
279	Bydgoszcz	RH117	64	pT2N0	IDC	2	UF	Luminal B	-	1(B)	1	2	1
280	Bydgoszcz	SE135	62	pT2N0	ILC	2	UF	Luminal B	-	1(B)	1	1	1
281	Bydgoszcz	SJ88	76	pT2N0	IDC	2	UF	Luminal B	-	1(B)	0	1	0
282	Bydgoszcz	SK58	68	pT2N0	IDC	2	UF	Triple neg.*		1(B)	1	1	0

<sup>1</sup> Tumor stage according to the TNM Classification of Malignant Tumors (TNM), 7<sup>th</sup> edition. ([uicc.org/resources/tnm](http://uicc.org/resources/tnm)).

<sup>2</sup> IDC = invasive ductal ca. , ILC = invasive lobular ca., DCIS= ductal ca. *in situ*, LCIS = lobular ca. *in situ*, IPC = invasive papillary ca., TLC = tubulo-lobular ca., IC= invasive ca., ICC=invasive cribriform ca.

<sup>3</sup> UF = unifocal, MF = multifocal.

<sup>4</sup> Molecular phenotypes according to the St. Gallen 2011 molecular subtypes classification. (Goldhirsch et al., *Annals of Oncology* 22: 1736-1747, 2011).

<sup>5</sup> HER2 status for luminal B molecular subtype cases: "-" = HER2 negative, "+" = HER2 positive.

<sup>6</sup> Genotyping experiments where performed on blood (B) or skin tissues (S), according to the control tissue availability.

\* Abbreviations used: comp.= component, ca. = carcinoma, Unclassif. = unclassified., Triple neg.= Triple negative

n.a. - data not available

**Supplemental Table 2. Summary of genetic and clinical data from 183 aberrant uninvolved margin samples (UM) in 108 individual patients, ordered by increasing total size of scored aberrations. The UM specimens with a total aberration load <=105.6 Mb are highlighted by grey background.**

Case ID	Sample ID	Tumor molecular phenotype <sup>1</sup>	Number of scored aberrations	Chromosomes involved in the aberrations <sup>2</sup>	Total size of scored aberrations <sup>3</sup> (Mb)	Candidate genes targeted by aberrations <sup>4</sup>	Comments	Distance of UM from the edge of nearest tumor (cm) <sup>5</sup>
1	MN036	MN036-UM6	Luminal B (HER2+)	2 (gains)	17, 17	0.4	<i>ERBB2</i>	3.4
2	MN036	MN036-UM98	Luminal B (HER2+)	1 (gain)	17	0.4	<i>ERBB2</i>	3.2
3	017KM	017KM-UM-IL	Luminal B (HER2-)	1 (gain)	7	0.5	<i>EGFR</i>	n.s.
4	MA018	MA018-UM98	HER2+	1 (gain)	17	0.7	<i>ERBB2</i>	5.2
5	AW020	AW020-UM4	Luminal B (HER2+)	2 (gains)	17, 17	0.7	<i>ERBB2</i>	5.6
6	017KM	017KM-UM-EL	Luminal B (HER2-)	1 (gain)	7	0.7	<i>EGFR</i>	n.s.
7	MN036	MN036-UM1	Luminal B (HER2+)	2 (gains)	17, 17	0.8	<i>ERBB2</i>	0.5
8	MA018	MA018-UM1	HER2+	1 (gain)	17	0.9	<i>ERBB2</i>	0.7
9	PM102	PM102B	Triple neg.	3 (gains)	17, 17, 17	1.2	<i>ERBB2</i>	6
10	MH016	MH016_UM4	Luminal B (HER2+)	2 (gains)	17, 17	1.5	<i>ERBB2</i>	1.5
11	GC147	GC147-UM-IU2	Luminal A	1 (gain)	15	1.5	<i>IGF1R</i>	5
12	023GC	023GC-VB	Luminal B (HER2+)	1 (gain)	17	1.8	<i>MIR21, VMP1</i>	1.5
13	053KS	053KS-VB	Unclassif.**	1 (gain)	7	1.8	<i>EGFR</i>	1.5
14	GS166	GS166-UM-EU1	Triple neg.	1 (gain)	7	1.9	<i>EGFR</i>	trisomy X*
15	GS166	GS166-UM-EU2	Triple neg.	1 (gain)	7	2.1	<i>EGFR</i>	trisomy X*
16	BMF005	BMF005_UM1	HER2+	1 (gain)	17	2.3	<i>ERBB2</i>	0.4
17	BMF005	BMF005_UM5	HER2+	1 (gain)	17	2.3	<i>ERBB2</i>	1.2
18	077EP	077EP-UM	Luminal B (HER2+)	2 (gains)	17, 17	2.4	<i>ERBB2</i>	n.s.
19	GC147	GC147-UM-IU1	Luminal A	2 (gains)	15, 15	2.9	<i>IGF1R</i>	5
20	089SD	089SD-VB	Triple neg.	1 (gain)	6	3.1	<i>MYB</i>	1.5
21	143DMG	143DMG-VB1	Luminal B (HER2-)	1 (gain)	11	3.7	<i>CCND1</i>	1
22	MD006	MD006-UM1	HER2+	3 (gains)	17, 17, 17	3.9	<i>ERBB2</i>	n.s.
23	017KM	017KM-UM-IU	Luminal B (HER2-)	2 (gains)	5, 7	4.6	<i>LIFR, EGFR</i>	n.s.
24	017KM	017KM-UM-EU	Luminal B (HER2-)	2 (gains)	5, 7	4.7	<i>LIFR, EGFR</i>	n.s.
25	EG163	EG163-UM-EL1	HER2+	4 (gains)	17, 17, 17, 17	5.3	<i>ERBB2, MIR21, VMP1</i>	n.s.
26	MW158	MW158-VB2-M	Luminal B (HER2-)	2 (gains)	15, 15	5.3	<i>IGF1R</i>	2
27	IP008	IP008-UM1	Luminal A	1 (gain)	8	5.5	<i>FGFR1</i>	0.2
28	NM48	NM48B	Luminal B (HER2+)	2 (gains)	17, 17	5.7	<i>ERBB2</i>	6
29	JD67	JD67B	Luminal B (HER2-)	3 (gains)	11, 11, 11	6.2	<i>CCND1</i>	6
30	AW020	AW020-UM3	Luminal B (HER2+)	4 (gains)	8, 8, 17, 18	7.4	<i>ERBB2</i>	1.4
31	MW158	MW158-UM-EU1	Luminal B (HER2-)	3 (gains)	15, 15, 15	7.4	<i>IGF1R</i>	n.s.
32	098WC	098WC-UM-IU	Luminal B (HER2-)	2 (gains)	8, 17	7.5	<i>MYC, NGFR</i>	4
33	EG163	EG163-VB2-M	HER2+	7 (gains)	17, 17, 17, 17, 17, 17, 17	7.8	<i>ERBB2, MIR21, VMP1</i>	3
34	021MB	021MB-UM-EL	Luminal B (HER2+)	4 (gains)	11, 11, 17, 17	8.1	<i>CCND1, ERBB2</i>	n.s.
35	EJ001	EJ001-UM1	Triple neg.	1 (CNNLOH)	11	8.6	<i>HRAS</i>	n.s.
36	EJ001	EJ001-UM2	Triple neg.	1 (CNNLOH)	11	8.6	<i>HRAS</i>	n.s.
37	EJ001	EJ001-UM3	Triple neg.	1 (CNNLOH)	11	8.6	<i>HRAS</i>	n.s.
38	EJ001	EJ001-UM99	Triple neg.	1 (CNNLOH)	11	8.7	<i>HRAS</i>	n.s.
39	EJ001	EJ001-UM98	Triple neg.	1 (CNNLOH)	11	9	<i>HRAS</i>	n.s.
40	EG163	EG163-VB1-M	HER2+	8 (gains)	17, 17, 17, 17, 17, 17, 17, 17	9.3	<i>ERBB2, MIR21, VMP1</i>	1.5
41	MW158	MW158-VB1-M	Luminal B (HER2-)	1 (gain)	15	9.3	<i>IGF1R</i>	1
42	ME114	ME114B	Luminal B (HER2+)	4 (gains)	8, 17, 17, 18	10	<i>ERBB2</i>	6
43	MD006	MD006-UM2	HER2+	5 (gains)	17, 17, 17, 17, 17	10.5	<i>ERBB2, MIR21, VMP1</i>	n.s.
44	MH047	MH047-UM3	Luminal B (HER2+)	8 (gains)	17, 17, 17, 17, 17, 17, 17, 19	12.4	<i>ERBB2</i>	2.7
45	131SD	131SD-UM-IL	Luminal A	1 (del)	7	13.7	<i>DMT1</i>	6
46	ZL152	ZL152-VB1-M	Luminal B (HER2+)	11 (gains)	4, 4, 9, 17, 17, 17, 19, 19, 19, 19, 22	13.8	<i>ERBB2, MIR21, VMP1, FGFR3, BCR</i>	1
47	077EP	077EP-VB	Luminal B (HER2+)	5 (gains)	16, 17, 17, 17, 17	16.9	<i>CREBBP, TSC2, ERBB2</i>	1.5

48	OH113	OH113B	Luminal B (HER2-)	2 (gains)	17, 17	18.1	<i>ERBB2, NGFR, MIR21, VMP1</i>	6	
49	DM138	DM138B	Luminal A	2 (gains)	8, 8	19.1	<i>MYC</i>	6	
50	GC147	GC147-VB1	Luminal A	4 (gains)	8, 15, 17, 17	19.3	<i>FGFR1, IGF1R</i>	1	
51	GGB040	GGB040-UM4	Luminal B (HER2-)	2 (gains)	8, 11	19.7	<i>MYC, CCND1</i>	0.4	
52	KK151	KK151-UM-EU	Luminal B (HER2+)	10 (gains)	7, 7, 7, 7, 7, 7, 7, 7, 7, 7	20.7	<i>BRAF</i>	4.5	
53	MW158	MW158-UM-EL2	Luminal B (HER2-)	1 (del)	3	23.7	<i>BAP1, FHIT</i>	n.s.	
54	KK123	KK123B	Luminal A	3 (1 gain, 2 CNNLOHs)	12, 9, 19	25.3	<i>MDM2</i>	6	
55	MN036	MN036-UM2	Luminal B (HER2+)	8 (gains)	6, 7, 7, 12, 17, 17, 17, 17	27.7	<i>FOXO3, PRDM1, MDM2, ERBB2, MIR21, VMP1</i>	0.4	
56	026MS	026MS-UM-IU	Triple neg.	1 (del)	13	32.3	<i>RB1, DACH1</i>	n.s.	
57	TP169	TP169-UM-EU1	HER2+	5 (gains)	6, 6, 12, 17, 17	35.9	<i>ERBB2, FOXO3, PRDM1, NGFR</i>	7	
58	012MC	012MC-VB	Luminal B (HER2+)	8 (gains)	1, 1, 12, 12, 17, 17, 17, 17	36.1	<i>ERBB2</i>	1.5	
59	MN036	MN036-UM5	Luminal B (HER2+)	13 (12 gains, 1 del)	6, 7, 7, 7, 7, 12, 17, 17, 17, 17, 17, 22	36.5	<i>FOXO3, PRDM1, EGFR, MDM2, ERBB2, MIR21, VMP1</i>	2.1	
60	099OLZ	099OLZ-VB	Triple neg.	2 (1 gain, 1 del)	8, 16	37.2		del 16q	1.5
61	MW158	MW158-UM-IU1	Luminal B (HER2-)	3 (gains)	15, 17, 19	39.1	<i>IGF1R, MIR21, VMP1</i>	n.s.	
62	GGB040	GGB040-UM1	Luminal B (HER2-)	4 (gains)	8, 11, 14, 17	39.7	<i>MYC, CCND1</i>	0.6	
63	GGB040	GGB040-UM3	Luminal B (HER2-)	3 (gains)	8, 11, 17	45.9	<i>MYC, CCND1</i>	1.9	
64	065AS	065AS-VB	Triple neg.	5 (gains)	6, 6, 6, 7, 9	46.3	<i>MYB, MET</i>	1.5	
65	141BB	141BB-VB1	Luminal B (HER2-)	1 (gain)	13	51.4	<i>ERCC5</i>	1	
66	ML36	ML36B2	Luminal B (HER2-)	3 (gains)	8, 8, 16	56.1	<i>FGFR1, MYC, PPP2R2A</i>	6	
67	KS141	KS141B	Triple neg.	3 (gains)	4, 4, 8	67.9	<i>MYC</i>	6	
68	MH047	MH047-UM2	Luminal B (HER2+)	7 (6 gains, 1 del)	6, 8, 8, 9, 17, 17, 17	74	<i>ERBB2, MIR21, VMP1, PPP2R2A</i>	0.5	
69	ML36	ML36B3	Luminal B (HER2-)	3 (gains)	8, 8, 16	82.7	<i>FGFR1, MYC</i>	6	
70	GGB040	GGB040-UM2	Luminal B (HER2-)	9 (8 gains, 1 CNNLOH)	6, 8, 8, 8, 11, 14, 17, 17, 17	83.9	<i>MYC, CCND1, MIR21, VMP1</i>	0.4	
71	MS168	MS168-UM-EU	Luminal B (HER2-)	3 (dels)	3, 14, 16	92.8		del 16q	7.5
72	EW155	EW155-UM-IL2	Luminal B (HER2-)	2 (1 gain, 1 del)	7, 16	98.6	<i>MET, BRAF</i>	4	
73	KZ54	KZ54B	Luminal B (HER2+)	1 (gain)	8	99.5	<i>MYC</i>	6	
74	025JT	025JT-UM-EU	Luminal B (HER2-)	1 (gain)	1	104.1		1q gain	n.s.
75	AL002	AL002_UM99	Luminal B (HER2+)	3 (gains)	8, 17, 19	104.4	<i>MYC, ERBB2, JAK3, CRTC1</i>	0.5	
76	095ESZ	095ESZ-VB	HER2+	3 (gains)	8, 17, 17	104.6	<i>MYC, ERBB2</i>	1.5	
77	SD164	SD164-UM-EL	Luminal B (HER2-)	1 (gain)	1	104.9		1q gain	5
78	130JT	130JT-VB2	Luminal B (HER2+)	1 (gain)	1	105.2		1q gain	2
79	043WB	043WB-VB	Luminal A	1 (gain)	1	105.6		1q gain	1.5
80	142AK	142AK-VB1	Luminal B (HER2+)	1 (gain)	1	105.6		1q gain	1
81	AL002	AL002_UM1	Luminal B (HER2+)	4 (gains)	8, 17, 17, 19	107.6	<i>MYC, ERBB2, JAK3, CRTC1</i>	0	
82	EW155	EW155-UM-IL1	Luminal B (HER2-)	2 (1 gain, 1 del)	7, 16	107.7	<i>MET, BRAF</i>	4	
83	063JB	063JB-UM-EU	Luminal B (HER2-)	2 (gains)	1, 8	109.8	<i>FGFR1</i>	2.5	
84	JU32	JU32B	HER2+	3 (gains)	5, 5, 8	111.4	<i>MYC</i>	6	
85	MD052	MD052-UM1	Luminal B (HER2-)	12 (gains)	7, 7, 7, 8, 8, 8, 8, 10, 10, 11, 11, 11	119.2	<i>BRAF, FGFR1, MYC, CCND1</i>	1.1	
86	AH028	AH028-UM3	Luminal B (HER2-)	7 (2 gains, 5 dels)	1, 1, 16, 16, 17, 17, 19	121.5	<i>MIR21, VMP1, JAK3, CRTC1, TP53</i>	0.5	
87	MW158	MW158-UM-IL	Luminal B (HER2-)	1 (CNNLOH)	11	135	<i>HRAS</i>	n.s.	
88	085AS	085AS-UM-EU	Luminal B (HER2-)	9 (gains)	8, 12, 12, 12, 13, 17, 17, 19, 19	141.7	<i>MYC</i>	24	
89	063JB	063JB-VB	Luminal B (HER2-)	4 (3 gains, 1 del)	1, 8, 8, 8	143.8	<i>FGFR1</i>	1.5	
90	013WS	013WS-UM-EU	HER2+	2 (1 gain, 1 del)	1, 16	147.7		1q gain, del 16q	n.s.
91	021MB	021MB-VB	Luminal B (HER2+)	2 (1 gain, 1 del)	1, 16	148.1		1q gain, del 16q	1.5
92	BD038	BD038-UM1	Luminal A	2 (1 gain, 1 del)	1, 16	148.8		1q gain, del 16q	0.3
93	133ML	133ML-VB1	Luminal B (HER2-)	2 (1 gain, 1 del)	1, 16	148.9		1q gain, del 16q	1
94	133ML	133ML-UM-EU	Luminal B (HER2-)	2 (1 gain, 1 del)	1, 16	149		1q gain, del 16q	4
95	LF042	LF042-UM3	Luminal A	2 (1 gain, 1 del)	1, 16	149.2		1q gain, del 16q	0.4
96	062BI	062BI-VB	Luminal A	2 (1 gain, 1 del)	1, 16	149.4		1q gain, del 16q	1.5
97	BD038	BD038-UM2	Luminal A	2 (1 gain, 1 del)	1, 16	149.9		1q gain, del 16q	0.8
98	049ASZ	049ASZ-UM-IU	Luminal A	2 (1 gain, 1 del)	1, 16	150		1q gain, del 16q	2
99	IMH013	IMH013_UM4	Luminal A	2 (1 gain, 1 del)	1, 16	150.6		1q gain, del 16q	0.9

100	054MJ	054MJ-UM	Luminal B (HER2-)	2 (1 gain, 1 del)	1, 16	150.7		1q gain, del 16q	3
101	HZK162	HZK162-UM-EL1	Luminal B (HER2-)	2 (1 gain, 1 del)	1, 16	150.7		1q gain, del 16q, trisomy X*	n.s.
102	ACV037	ACV037-UM1	Luminal B (HER2+)	7 (gains)	11, 17, 17, 17, 17, 8	153.9	<i>FGFR1, MYC, ERBB2</i>		0.6
103	LK003	LK003_UM1	Luminal A	4 (3 gains, 1 del)	1, 11, 14, 16	154.8		1q gain, del 16q	1.3
104	BD038	BD038-UM3	Luminal A	3 (1 gain, 2 dels)	1, 12, 16	157		1q gain, del 16q	0.6
105	HS006	HS006-UM1	Luminal A	3 (2 gains, 1 del)	1, 15, 16	158.2		1q gain, del 16q	0.4
106	CG010	CG010_UM2	Unclassif.**	4 (gains)	1, 5, 17, 17	159.3	<i>LIFR, ERBB2</i>		0
107	078AW	078AW-UM-IL	Luminal B (HER2+)	11 (6 gains, 5 dels)	11, 11, 11, 11, 11, 11, 11, 11, 11, 16, 16, 22	162.6	<i>CREBBP, TSC2, ATM, RBFOX2</i>		3
108	133ML	133ML-VB2	Luminal B (HER2-)	2 (1 gain, 1 del)	1, 16	164.1		1q gain, del 16q	2
109	013WS	013WS-VB	HER2+	3 (1 gain, 1 del, 1 CNNLOH)	1, 16, 17	168.6		1q gain, del 16q	n.s.
110	KM159	KM159-UM-IU1	Luminal A	8 (7 gains, 1 del)	8, 11, 11, 11, 11, 11, 16, 1	173.1	<i>FGFR1, CCND1</i>		n.s.
111	139MD	139MD-VB1	Luminal B (HER2-)	3 (2 gains, 1 del)	1, 16, 16	182.7	<i>CREBBP, TSC2</i>		1
112	MK120	MK120B	Luminal A	3 (2 gains, 1 del)	1, 16, 16	185.8	<i>CREBBP, TSC2</i>		6
113	BU97	BU97B	Triple neg.	7 (6 gains, 1 CNNLOH)	3, 7, 8, 12, 17, 18, 22	187.1	<i>MYC, MIR21, VMP1</i>		6
114	AW020	AW020-UM2	Luminal B (HER2+)	12 (10 gains, 2 dels)	3, 4, 6, 6, 6, 8, 8, 8, 17, 17, 18, 19	191.1	<i>ERBB2, JAK3, CRTC1, SETD2, BAP1, ATRIP, RASSF1, FHIT</i>		0.3
115	100AW	100AW-UM-IU	Luminal B (HER2-)	4 (2 gains, 2 dels)	8, 8, 16, 16	192.8	<i>FGFR1, CREBBP, TSC2, PPP2R2A</i>		3
116	KK151	KK151-UM-IU1	Luminal B (HER2+)	9 (7 gains, 2 dels)	1, 3, 7, 7, 7, 16, 20, 21, 21	193.6	<i>BRAF, SETD2, BAP1, ATRIP, RASSF1, FHIT</i>		5
117	RH117	RH117B	Luminal B (HER2-)	11 (8 gains, 3 dels)	1, 8, 8, 8, 8, 11, 11, 11, 11, 11, 22	197.6	<i>FGFR1, CCND1, PPP2R2A, RBFOX2</i>		6
118	AH028	AH028-UM5	Luminal B (HER2-)	12 (2 gains, 10 dels)	1, 3, 4, 12, 13, 16, 16, 16, 17, 19, 19, 21	200.3	<i>JAK3, CRTC1, TP53</i>		0.6
119	KK151	KK151-UM-EL2	Luminal B (HER2+)	3 (1 gain, 2 dels)	16, X, 11	214	<i>CCND1</i>		4
120	037MC	037MC-UM-IU	Luminal A	3 (1 gain, 2 dels)	1, 6, 6	277.7		1q gain	n.s.
121	061AS	061AS-VB	HER2+	8 (6 gains, 1 del, 1 CNNLOH)	1, 6, 12, 16, 17, 17, 17, 17	294	<i>FOXO3, PRDM1, ERBB2</i>		1.5
122	AE031	AE031-UM3	Luminal A	2 (1 gain, 1 del)	1, 4	296		1q gain	0
123	049ASZ	049ASZ-VB	Luminal A	3 (2 gain, 1 del)	1, 16, X	306.2		1q gain, del 16q	1.5
124	ML36	ML36B	Luminal B (HER2-)	7 (3 gains, 4 dels)	8, 8, 8, 10, 16, 16, 16	312.7	<i>FGFR1, MYC, CREBBP, TSC2</i>		6
125	DH74	DH74B	Triple neg.	5 (4 gains, 1 CNNLOH)	1, 3, 3, 12, 13	316.7		1q gain	6
126	095ESZ	095ESZ-UM-EU	HER2+	8 (6 gains, 2 dels)	1, 1, 5, 8, 8, 17, 17, 17	317.3	<i>LIFR, MYC, ERBB2, ARID1A, PPP2R2A</i>		2.5
127	LH045	LH045-UM3	Luminal A	9 (1 gain, 8 dels)	1, 4, 11, 16, 17, 17, 22, 22, X	344.7	<i>ATM, TP53, RBFOX2</i>		0.8
128	139MD	139MD-VB2	Luminal B (HER2-)	5 (3 gains, 2 dels)	1, 5, 8, 16, 16	348.5	<i>FGFR1, MYC, CREBBP, TSC2</i>		2
129	AL002	AL002_UM2	Luminal B (HER2+)	9 (6 gains, 2 dels, 1 CNNLOH)	1, 8, 11, 12, 17, 17, 19, 19, 22	364.2	<i>MYC, ERBB2, JAK3, CRTC1</i>		0
130	LH045	LH045-UM1	Luminal A	13 (1 gain, 12 dels)	1, 5, 5, 11, 11, 11, 11, 16, 17, 17, 22, 22, X	372.5	<i>ATM, TP53, RBFOX2</i>		0.2
131	LH045	LH045-UM2	Luminal A	9 (1 gain, 8 dels)	1, 5, 5, 11, 16, 17, 17, 22, X	373.2	<i>ATM, TP53, RBFOX2</i>		0.2
132	GS011	GS011-UM2	Luminal B (HER2-)	10 (5 gains, 5 dels)	2, 5, 6, 8, 11, 11, 11, 16, 16, 18	384.3	<i>CCND1, ATM</i>		0.7
133	ML012	ML012-UM2	Luminal A	8 (2 gains, 6 dels)	1, 1, 8, 9, 9, 16, 16, 17	398.3	<i>CREBBP, TSC2, ARID1A, PPP2R2A, TP53</i>		0
134	KB132	KB132B	Luminal B (HER2-)	14 (10 gains, 3 dels, 1 CNNLOH)	1, 1, 3, 5, 6, 6, 6, 6, 7, 8, 8, 8, 16, 18	417	<i>FGFR1, DMTF1</i>		6
135	BMK015	BMK015_UM1	Luminal A	15 (8 gains, 7 dels)	1, 1, 1, 7, 8, 12, 13, 13, 13, 13, 13, 13, 14, 16, X	445.9	<i>EGFR, MET, BRAF, ARID1A, RB1, DACH1</i>		0.3
136	017KM	017KM-VB	Luminal B (HER2-)	5 (2 gains, 3 dels)	1, 16, 17, 18, 1	446.5	<i>TP53</i>		1.5
137	ML012	ML012-UM1	Luminal A	8 (3 gains, 5 dels)	1, 1, 8, 8, 9, 16, 16, 17	466.8	<i>MYC, CREBBP, TSC2, ARID1A, PPP2R2A, TP53</i>		0
138	100AW	100AW-UM-EU	Luminal B (HER2-)	7 (3 gains, 4 dels)	1, 5, 8, 8, 16, 16, 18	475.2	<i>FGFR1, MYC, CREBBP, TSC2, PPP2R2A</i>		5
139	037MC	037MC-VB	Luminal A	8 (3 gains, 5 dels)	1, 6, 6, 8, 13, 16, 16, 22	475.9	<i>CREBBP, TSC2, RB1, DACH1, RBFOX2</i>		1.5
140	UV023	UV023-UM1	Luminal A	7 (2 gains, 5 dels)	1, 6, 11, 11, 13, 13, 16	482.6	<i>CCND1, ATM, RB1, DACH1</i>		0.3
141	UV023	UV023-UM5	Luminal A	7 (3 gains, 4 dels)	1, 6, 11, 11, 13, 13, 16	484.4	<i>CCND1, ATM, RB1, DACH1</i>		1.2
142	KK151	KK151-UM-EU2	Luminal B (HER2+)	16 (11 gains, 5 dels)	1, 2, 3, 6, 7, 7, 7, 7, 7, 7, 7, 11, 11, 12, 14	486.5	<i>FOXO3, PRDM1, MYB, BRAF, SETD2, BAP1, ATRIP, RASSF1, FHIT</i>		4.5
143	100AW	100AW-VB	Luminal B (HER2-)	10 (5 gains, 5 dels)	1, 8, 8, 8, 11, 11, 11, 16, 16, 18	532.8	<i>MYC, CCND1, CREBBP, TSC2, PPP2R2A, ATM</i>		1.5
144	011BM	011BM-VB	Luminal B (HER2-)	12 (6 gains, 6 dels)	1, 1, 4, 6, 9, 10, 11, 11, 11, 11, 16, 17	548.9	<i>CCND1, CREBBP, TSC2, ARID1A, ATM, TP53</i>		1.5



173	071ZB	071ZB-VB	Triple neg.	not scored <sup>6</sup>	numerous	>39% of the genome	1.5
174	075JS	075JS-VB	Luminal B (HER2-)	not scored <sup>6</sup>	numerous	>39% of the genome	1.5
175	089SD	089SD-UM-IU	Triple neg.	not scored <sup>6</sup>	numerous	>39% of the genome	12
176	098WC	098WC-VB	Luminal B (HER2-)	not scored <sup>6</sup>	numerous	>39% of the genome	1.5
177	129EB	129EB-VB1	Luminal B (HER2-)	not scored <sup>6</sup>	numerous	>39% of the genome	1
178	138BM	138BM-S-VB2	Luminal B (HER2-)	not scored <sup>6</sup>	numerous	>39% of the genome	2
179	141BB	141BB-UM-EU	Luminal B (HER2-)	not scored <sup>6</sup>	numerous	>39% of the genome	4
180	141BB	141BB-VB2	Luminal B (HER2-)	not scored <sup>6</sup>	numerous	>39% of the genome	2
181	JP149	JP149-UM-EU2	Triple neg.	not scored <sup>6</sup>	numerous	>39% of the genome	3
182	KS150	KS150-VB1-M	Luminal B (HER2-)	not scored <sup>6</sup>	numerous	>39% of the genome	1
183	SD164	SD164-UM-EU1	Luminal B (HER2-)	not scored <sup>6</sup>	numerous	>39% of the genome	3.5

<sup>1</sup> Molecular phenotypes according to the St. Gallen 2011 molecular subtypes classification (Goldhirsch *et al.*, Annals of Oncology 22: 1736-1747, 2011).

<sup>2</sup> Each entry in this column indicates a distinct scored aberration on a chromosome. Repeated entry of the same chromosome number indicates a distinct call.

<sup>3</sup> The total combined length of all scored aberrations in million base pairs (Mb). The cells shaded in grey indicate UM samples with total aberration load that is consistent with normal cell morphology.

<sup>4</sup> The gene symbols are color coded according to the type of underlying aberration: blue - gain; green - copy number neutral LOH (UPD); and red - deletion.

<sup>5</sup> The distance between the primary tumor and UM sample was measured "edge to edge". For patients with multifocal disease, the distance was measured to the closest primary tumor. n.s. - not specified

In six instances of UM samples from Falun-clinic, the microscopic reinvestigation of large-scale histology preparations resulted in detection of tumor cells in the area where UM-samples were taken (indicated by zero-distance from the primary tumor).

<sup>6</sup> Pronounced cancer-like genome profile, with numerous aberrations difficult to size precisely.

\* Constitutional trisomy X (verified in the samples from normal control tissue).

\*\* Unclassif. = Unclassified molecular phenotype

Supplemental Table 3. Frequency of low copy number gains of six growth factor receptor genes in subjects and UMs stratified by total genomic size of scored aberrations: <39% of the whole genome and combined total size <= 105.6 Mb.

	Subjects with UMs containing scored aberrations covering <39% of the whole genome		Subjects with UMs containing total scored aberrations <= 105.6 Mb	
	in 156 UMs	in 93 subjects	in 80 UMs	in 50 subjects
<b>A Gain frequency of each receptor gene *</b>				
<i>ERBB2</i>	30.1% (n=47)	31.2% (n=29)	38.75% (n=31)	44% (n=22)
<i>LIFR</i>	3.8% (n=6)	5.4% (n=5)	2.5% (n=2)	6% (n=3)
<i>EGFR</i>	7.1% (n=11)	7.5% (n=7)	10% (n=8)	10% (n=5)
<i>FGFR1</i>	10.3% (n=16)	12.9% (n=12)	5% (n=4)	14% (n=7)
<i>IGF1R</i>	5.1% (n=8)	3.2% (n=3)	8.75% (n=7)	8% (n=4)
<i>NGFR</i>	6.4% (n=10)	8.6% (n=8)	3.75% (n=3)	20% (n=10)
<b>B Gain of multiple receptor genes in a single UM or in the same subject</b>				
>=1 receptor	48.1% (n=75)	49.5% (n=46)	61.25% (n=49)	60% (n=30)
>=2 receptors	10.9% (n=17)	19.4% (n=18)	7.5% (n=6)	20% (n=10)
>=3 receptors	3.2% (n=5)	7.5% (n=7)	-	8% (n=4)
>=4 receptors	0.6% (n=1)	3.2% (n=3)	-	6% (n=3)
>=5 receptors	-	-	-	-
6 receptors	-	-	-	-
<b>C Coexistence of gain of <i>ERBB2</i> with each of the other five additional receptor genes</b>				
<i>ERBB2</i> + <i>LIFR</i>	n.a.	4.3% (n=4)	n.a.	4% (n=2)
<i>ERBB2</i> + <i>EGFR</i>	n.a.	3.2% (n=3)	n.a.	4% (n=2)
<i>ERBB2</i> + <i>FGFR1</i>	n.a.	3.2% (n=3)	n.a.	8% (n=4)
<i>ERBB2</i> + <i>IGF1R</i>	n.a.	1.1% (n=1)	n.a.	4% (n=2)
<i>ERBB2</i> + <i>NGFR</i>	n.a.	7.5% (n=7)	n.a.	10% (n=5)

\* Numbers shown are not taking into account coexistence of gains for several receptor genes in the same UM sample/subject. Abbreviations used: "n.a." - not applicable; "-" - no multiple gene receptor gains in this category.